



Attenuation of Gamma Rays in New Concrete Forms

(RB2C Enhancement Project)
GRANCRETE, INC.

Mohamed Bourham¹ and Sami Riskalla²

¹Department of Nuclear Engineering

*²Department of Civil, Construction and Environmental Engineering
North Carolina State University
Raleigh, NC 27695*

Contributors

Dr. Mervat Khalil

Housing & Building National Research Center
Building Physics and Environment Institute, Egypt

Leigh Winfrey and Joshua Nowak

*Department of Nuclear Engineering
North Carolina State University
Raleigh, NC 27695-7909*

Testes were performed in the Ray Murray Radiation Laboratory in the Department of Nuclear Engineering, North Carolina State University, Raleigh, NC 7695-7909

January 20, 2010

Table of Contents

Cover Page	1
Table of Contents	2
1. Introduction	3
2. Background	3
3. Radiation Interaction	5
4. Attenuation of Radiation	7
5. Materials of Radiation Shielding Concrete	8
6. Design of Concrete for Radiation Shielding	11
7. Experimental Measurement of γ -ray Attenuation in Grancrete™ Concretes Product GCI 2000	12
7.1 Experimental Setup	12
7.2 Experimental Results of Grancrete™ Groups A and B	13
7.2.1 Test Results on the Attenuation of γ -Rays “Group A”	13
7.2.2 Test Results on the Attenuation of γ -Rays “2 nd Group A”	18
7.2.3 Test Results on the Attenuation of γ -Rays “Group B”	24
8. Remarks on Grancrete™ Groups A and B results	30
8.1. Remarks for 1 st group of group (A)	30
8.2. Remarks for 2 nd group of group (A)	30
8.3. Remarks for group (B)	31
9. Test Results on the Attenuation of γ -Rays Composed HFR Samples	31
9.1 Experimental Setup	31
9.2 Grancrete™ HFR Samples	34
9.3 Experimental Results of Grancrete™ HFR Samples	35
9.4 Remarks for HFR Samples	37
9.5 Thickness Calculations and measured Densities of HFR Samples	39
10. Experimental Results of Grancrete™ GCI Samples	40
10.1 Experimental Results	41
10.2 Remarks for GCI Samples	43
11. Investigation of Magnetization Effects of Molded Grancrete Composed Concretes	44
11.1 Introduction	44
11.2 Samples Tested for Magnetization	45
11.3 Magnetization Experimental Arrangement	46
11.4 Magnetization Test Results	47
11.5 Remarks on Magnetization Test Results	48
References	49
Appendix 1: Physical and Mechanical Properties of Test Groups (A) and (B)	51
Appendix 2: Photograph of sample 7B with observed cracking	66
Appendix 3: Photographs of different samples after compressive stress test	67

1- Introduction

Radiation shielding serves a number of functions, among these is reducing the radiation exposure to persons in the vicinity of radiation sources. Shielding used for this purpose is known as 'biological' shielding. Shields are also used in reactors to reduce the intensity of gamma rays incident on the reactor vessel, which protect the vessel from excessive heating due to gamma ray absorption and reduce radiation damage due to neutrons. These shields are also known as thermal shields. Shielding is also necessary for disposal of nuclear waste, low-level waste such as short-lived nuclides and radioactive materials used in research, medicine and biological experiments, and high-level waste such as nuclear spent fuel.

The main purpose of radiation shielding is to reduce the intensity of external radiation to the desired *acceptable* level. The attenuation properties of a shielding material are of prime concern. There are many other factors of mechanical and economic nature, which must also be considered in the choice of materials for radiation shielding. Different materials may achieve the desired reduction in radiation intensity if a sufficient thickness is used. However, excessive thickness may not be desirable because of space considerations and increased costs. Concrete is considered an excellent and versatile shielding material and is widely used for the shielding of nuclear power plants, particle accelerators, research reactors, laboratory hot cells, radiation and x-ray medical facilities, and nuclear waste casks. It is relatively inexpensive, could be fabricated into complex shapes and can easily be handled. It contains a mixture of many light and heavy elements and therefore has good attenuation of photons and neutrons. By varying its composition and density the shielding characteristics of concrete may be adapted to a wide range of use.

Concrete has also good structural properties which is a factor of importance in large stationary installations such as nuclear power plants. Although has some disadvantages such as low thermal conductivity, which may cause high temperature gradients and thermal stresses, it is in many respects considered to be an ideal shielding material and is probably the most versatile and widely used materials for this purpose (M.F. Kaplan, 1989).

2- Background

Exposure to radiation comes from various sources such as cosmic rays, highly energetic radiation from outer space and terrestrial natural radiation. Natural radiation included naturally-radioactive elements. Additional radiation sources are x-rays in medical facilities, nuclear reactors, nuclear weapons, cathode ray tubes used in TV and computer displays, and numerous other radiation-producing devices. Magnitude of the radiation dose in any radiation-producing facility, as well as natural sources, must be controlled to eliminate exposure to radiation, or to limit exposure to the regulatory standards (J.R. Lamarsh, 2001). In all cases, the central problem is to determine the

thickness and/or composition of shielding material required to reduce biological dose rate to predetermined *acceptable* levels. The shielding is determined by the nature of the facility and the maximum doses produced, thus attenuation of radiation is an important subject for the safety of personnel and the environment.

Buildings are constructed mostly using concretes containing water, cement and aggregates. In a building construction, two main points have to be considered. They are resistance against earthquake expressed as strength of the building, and resistance against radiation expressed as radiation attenuation. Using of barite (BaSO_4) in building construction surely would be ideal to protect against radiation, but this is not feasible as there is not enough barite reserve in the world. Moreover the barite itself can't be used as a construction material in building. Thus, barite-loaded heavy concrete is one be used a construction materials in building for applications such as nuclear power plants, accelerators, hospitals, etc. Gamma-ray can easily penetrate into matter where; it is uncharged and has no mass, so the shielding of photons is very difficult. The interaction of γ rays depends on the incoming photon energy (I. Akkurt et al., 2005). The linear attenuation coefficient (μ), which is defined as the probability of a radiation interacting with a material per unit path length, is the most important quantity characterizing the penetration and diffusion of gamma radiation in a medium. The magnitude of linear attenuation coefficients depends on the incident photon energy, the atomic number and density (ρ) of the shielding materials (J. wood, 1982). As the linear attenuation coefficient (μ) depends on the density, it expressed as a mass attenuation coefficient which is the linear attenuation coefficient per unit mass of the material.

Materials used as biological shielding should have high attenuation coefficient and the effect of irradiation on its mechanical and optical properties should be small or negligible. In general, different concretes are used for gamma rays shield design but considerable variations in their compositions and water contents add uncertainty to the calculation of radiation attenuation coefficient (N. Singh et al., 2006). Several works have been performed to obtain linear attenuation coefficient (μ) for different elements (B. Goswami and N. Chaudhari, 1973), compounds (N. Singh et al., 1996 and U. Turgut et al., 2002) and alloys (El-Kateb et al., 2000). With the advancement of technology, there is a constant need to develop materials which can be used under a hostile environment of high radiation exposure and can be act as good radiation shield (J.F. Krocher and R.E. Browman, 1984). Measurement of mass attenuation coefficient began with the beginning of 20 century (N. Singh et al., 2006). First compilation of (μ/ρ) was provided by (S.J.M. Allen, 1935), and followed by published tables for 24 elements for photon energies in the region of 102.2 KeV to 6.13 KeV (C.M. Davison and R. D. Evens, 1952). NIST entered the area of collection, evaluation, analysis and compilation of (μ/ρ) data with the work of more researchers ended by (G.R. White Grodstein, 1957). New theories and measurements were incorporated by (J.H. Hubbell and M.J. Berger, 1968). Tables of mass attenuation coefficients and mass energy absorption coefficients for 40 elements and 45 mixture and compounds over the energy range from 1 KeV to 20 MeV were calculated (J.H. Hubbell, 1982). Later on, these tables were followed by development of XCOM computer program for calculating cross-section and attenuation coefficients for elements , compounds and mixture at photon energy from 1KeV to

100GeV (M. J. Berger and J. H. Hubbell , 1987). Extensive new calculation and theoretical tabulations of scattering cross-section and quantities related to mass attenuation coefficient have recently become available for photon energies from a few eV to 1MeV (or less), for Z=1 to Z= 92 (Chantler, 1995).

Yang et al., 1987 studied gamma rays and x-rays attenuation for biological material. Several theoretical and experimental works have been performed to obtain linear attenuation coefficient (μ) for building materials (I.I. Bashter, 1996; I.I. Bashter et al., 1996; A.S. Makarous et al., 1996; I.I. Bashter, 1997; I. Akkurt et al, 2004; and I. Akkurt et al, 2005); and for shielding concretes (A. S. Makarious et al., 1988; A. El-Sayed Abdo 2002; A. El-Sayed Abdo et al, 2003; A. El-Sayed Abdo et al, 2003). Other work carried out with polymer cement plaster to prevent the radon gas contamination (M. I. Awadallah, 2007 and X.F. Gao 2002). More studies were carried out with fiber concrete to investigate and modify the strength of concrete using carbon fiber (CF), (U.S. Camli and B. Binici, 2007) glass fiber (GF) (B. Benmokrane et al, 1995; R. Griffiths and A. Ball, 2000; J. M. L. Reis and A.J.M Ferreira, 2003), hybrid fiber (HPFC) (A. Hosny et al., 2006). But there is no study to investigate their effect on the linear attenuation coefficient of γ -ray.

In this study, under a contract with **RB2C for Grancrete™** concrete, the linear attenuation coefficient (μ) was measured and investigated for different **Grancrete™** concrete mixture to be used as shielding materials.

3- Radiation Interaction

About 340 nuclides are found in nature, and about 70 of them are naturally radioactive (normally in heavy elements), all elements with atomic number > 83 are radioactive. Some light elements are naturally radioactive, such as tritium, beryllium-10 and carbon-14. Some of the combinations of protons and neutrons are not stable. This is usually the case when the combination has too few or too many neutrons for the number of protons. To become more stable, the atom may release some of its extra energy by emitting radiation. The three basic types of radiation are alpha, beta and gamma.

Alpha (α) radiation is made of particles. These particles are made of two protons and two neutrons. Therefore an alpha particle is a Helium nucleus. This is the heaviest (about 4 atomic mass unit (amu)) of the radiations and has an electrical charge of +2. The range of alpha particles in air is about 2.5 cm for alpha particles with energy of 4MeV and about 7.3 cm for 8MeV alphas. In aluminum, it is about 0.015 and 0.055 cm for 4 and 8 MeV, respectively.

Beta (β) radiation is also made of particles. These particles are identical to normal electrons. They originate from the nucleus of the atom, not the group of electrons surrounding the atom. They are lighter than alphas and have a charge of -1. The range of beta particles is about 500 times that of alphas. In air, it is about 1.5 meters for 0.5MeV and 8.5 meters for 2MeV betas. In aluminum, it is about 6.5 mm and 4 cm for 0.5 and 2MeV betas, respectively.

Gamma (γ) radiation is electromagnetic radiation made of photons and is similar to X-rays, microwaves, light and radio waves. Gammas have no weight but they do carry energy and momentum, just like any other photon from the electromagnetic (EM) spectra. γ -rays are not particles and thus the mechanism of γ -interaction is different than α 's and β 's:

- Photoelectric Effect:

Here, gamma provides all its energy to eject an electron from the atom's inner shell, and the ejection of electron causes ionization.

- Compton Scattering:

Here, only part of gamma energy is consumed to eject an electron from the outer shell and a photon is scattered. This is the predominant mechanism for gammas in the energy range 1-2MeV.

- Pair Production:

Here, energy is converted to mass, gamma's energy is totally consumed and electron-positron pair appears. This can only occur for γ -energy > 1.02 MeV. (1.02 MeV = mass of 2 electrons, or the mass of an electron and a positron)

γ attenuates into matter by the exponential law:

$$I_{(x)} = I_{(o)} e^{-\mu x}$$

Where $I_{(x)}$ is the intensity of gamma after passing a material of thickness (x), $I_{(o)}$ is the intensity before passing through the material and μ is the linear attenuation coefficient. More precisely, μ is the summation of all attenuations due to γ -interactions, hence

$$\mu = \sum \mu_{all} = \mu_{photoelectric} + \mu_{Compton} + \mu_{pair\ production}$$

Biological effects are determined by the absorption of ionizing radiation in tissues. Indeed it differs between exposures to alpha, beta or gamma radiation. The range of absorption into materials is determined by the coefficient of absorption, or in other words, the attenuation coefficient. The Relative Biological Effectiveness (RBE) of a given radiation is an empirically derived term that, in general, all other factors are held constant, increases with the level of exposure in tissue in KeV/ μ m. The radiation becomes less efficient beyond approximately 100keV/ μ m. This is the result of overkill in which the maximal potential damage has already been reached, and the further increase beyond this point results in wasted dose. For example, at 500 KeV/ μ m many of

the cells may have three or more ionizing events when only two are required to kill the cell. Exposure to ionizing radiation has various effects on chromosomes, it may cause break in one chromosome resulting in centric and acentric fragments, ring formation resulting from two breaks in the same chromosome, translocation when two chromosomes suffer one break and the acentric fragment of one chromosome combines with the centric fragment and vice versa, or the two centric fragments recombine with each other at their broken ends, thus resulting in the production of dicentrics.

4- Attenuation of Radiation

The interaction of radiation with matter is stochastic in nature. The probability of an atomic particle or photon interacting in particular way with a given material per unit path length is called the Linear Attenuation Coefficient (μ). This attenuation coefficient is of great important in matters concerning radiation shielding and its dimension is cm^{-1} or 10^2m^{-1} . Linear attenuation coefficient is dependent on the density (ρ) of the shielding material. The density often does not have a unique value but depends on the physical state of the material (example: moisture content of concrete). To obviate the effects of variations in the density of a material, the linear attenuation coefficient is for reference purposes expressed as a mass attenuation coefficient (μ/ρ) $\text{cm}^2 \text{g}^{-1}$ and it is the direct measure of the effectiveness of a shielding material based upon unit mass of material. For shielding materials consisting of chemical compounds or homogeneous mixtures, the linear and mass attenuation coefficient can be obtained from the coefficients for the constituent elements according to the weighted average.

$$\mu = \sum \mu_i = \sum n_i \sigma_i \quad (1)$$

$$\frac{\mu}{\rho} = \sum w_i \left(\frac{\mu}{\rho_i} \right) \quad (2)$$

Where, w_i is the proportion by weight of the i^{th} constituent

μ is the linear attenuation coefficient

n_i is the number of atoms per unit volume

σ_i is the microscopic cross-section

ρ_i is the bulk density

Thus the mass attenuation coefficient of a composition such as ordinary concrete mix may be calculated as follows

$$\frac{\mu}{\rho} = \left(\frac{\mu}{\rho} \right)_{\text{element}(\text{cm}^2/\text{g})} \times \text{proportion by weight}$$

5- Materials of Radiation Shielding Concrete

The main purpose of radiation shielding is to reduce the intensity of external radiation to the standard acceptable level. The nuclear or attenuation properties of a shielding material is therefore of prime concern. There are many other factors of mechanical and economic nature, which must be considered in the choice of materials for radiation shielding. Many different kinds of materials may achieve the desired reduction in radiation intensity if a sufficient thickness is used. Excessive thickness may however be precluded because of space considerations, which may cause practical difficulties and increased cost. Different materials may on the other hand require smaller thicknesses but are not suitable for other reasons.

Concrete is considered to be an excellent and versatile shielding material and is widely used for the shielding in nuclear power plants, particle accelerators, research reactors, laboratory hot cells, nuclear waste containers and medical facilities. It is a relatively inexpensive material which may be easily handled and cast into complex shapes. It contains a mixture of many light and heavy elements and therefore has good nuclear properties for the attenuation of photons and neutrons. By varying its composition and density the shielding characteristics of concrete may be adapted to a wide range of use. Concrete has also good structural properties, which is a factor of importance in large stationary installations such as nuclear power plants and waste sites. Although concrete has some disadvantages such as low thermal conductivity, which may cause high temperature gradients and thermal stresses, it is in many respects considered to be an ideal shielding material and is probably the most versatile and widely used material for this purpose. In broad terms, concrete consists of aggregates bound together with cement, and the properties of these materials are considered for radiation shielding effectiveness.

A- Cement Types

Different types of cement may be used in concretes for radiation shielding, such as Portland cement, high alumina cement, and several kinds of special cements.

Portland cement

Portland cement is manufactured primarily from calcareous materials such as limestone or chalk, and from silica and alumina which is found as clay or shale. These materials are intimately mix and then burnt at a temperature of approximately 1400°C to form a clinker, which is then ground into a fine powder with the addition of gypsum to control the setting time. The main compounds of Portland cement are:

Tricalcium silicate	$3\text{CaO} \cdot \text{SiO}_2$
Dicalcium silicate	$2\text{CaO} \cdot \text{SiO}_2$
Tricalcium aluminate	$3\text{CaO} \cdot \text{Al}_2\text{O}_3$
Tetracalcium aluminoferrite	$4\text{CaO} \cdot \text{Al}_2\text{O}_3 \cdot \text{Fe}_2\text{O}_3$

In the presence of water the Portland cement compounds hydrate. The water content of hydrate past depends on the environmental temperature and it is estimated

that at room temperatures the water content is between 13 and 16 % by weight of the hydrated cement, i.e. approximately 0.3 g/cm^3 . The water content of hardened cement is of importance in that it provides a large portion of the hydrogen, which may be an advantage in radiation shielding. Various types of Portland cement are available and their physical characteristics differ depending mainly on their chemical composition.

High alumina cement

High alumina cement is made from bauxite and limestone or chalk. This cement typically contain between 37 and 41% by weight of alumina compared with 3 to 8% for Portland cements. the calcium Oxide content of high alumina cement is generally between 36 and 40% whereas for Portland cement it is between 60 and 76%. The amount of water required for the hydration of high alumina cement is about twice as much as that required for the hydration of Portland cement If hydration occurs at temperatures less than 30°C , the water content of the hydrated cement may be as high as 0.7 g/cm^3 , which is advantageous in regard to the neutron shielding properties of concrete made from this cement. One of the main problems of high alumina cement is the conversion of one form of calcium aluminates hydrate to another at elevated temperatures, which results in a loss in strength of the hardened cement past.

Several kinds of special cements

The main reason for considering the use of special cements for radiation shielding concrete is to increase the chemically bond water content because of the desirable properties of hydrogen for neutron shielding (moderation). Examples of these kinds are:

- Gypsum –alumina cement
- Magnesium Oxychloride Cement
- Magnesis cement
- Phosphate cement
- Oxyacid cement

B- Aggregates

Aggregate usually constitute at least 75% of the volume of concrete and they therefore have an important effect on its properties. Concrete for radiation shielding generally contains ordinary normal weight aggregates. Special types of aggregate are also used to improve the attenuation properties of concrete or to reduce the thickness of concrete shields.

Ordinary Normal-Weight Aggregates

Aggregate for ordinary concrete usually consists of sand, gravel or crushed aggregate from local sources. They are normally calcareous or siliceous minerals which occur in nature and which have a specific gravity (S.G.) between 2.5 and 2.7 .The density of ordinary Portland cement concrete made with these aggregates is generally between 2.2 and 2.4 g/cm^3 .

Special Aggregate

Special aggregate for radiation shielding concrete are either natural mineral aggregate or synthetic aggregates. Special natural mineral aggregate are used to attenuate photons, they are mainly heavy mineral ores such as barites magnetite, ilmenite and hematite, which have S.G. range from 4.0 to 4.8 g/cm³. For the attenuation of neutrons, natural hydrous aggregates are used such as bauxite, serpentine, goethite and limonite, as well as boron additives in the form of calcium borates. Synthetic aggregate are also used to produce concrete of high density, for example ferrophosphorus (S.G. 5.8 to 6.3 g/cm³), ferrosilicon (S.G. 6.5 to 7.0 g/cm³) and metallic iron product such as sheared metal bars, steel punching and iron shot, which have S.G. ranging from 7.5 to 7.8 g/cm³. Standard specification for aggregates for radiation shielding concrete (ASTM C637) covers special aggregates for radiation shielding concretes in which composition or high specific density or both are of prime consideration. Special aggregate which have been used for radiation shielding concrete are listed below:

Hydrous Aggregate

This aggregate used for slowing down or attenuation of fast or intermediate neutrons in a concrete shield, the hydrogen content of concrete may be increased by the inclusion of hydrous aggregates in the concrete mix, like; Serpentine (3MgO.2SiO₂.2H₂O), Limonite (2Fe₂O₃.3H₂O), Goethite (Fe₂O₃.H₂O), and Bauxite (Al₂O₃.2H₂O)

Heavy Aggregate

Heavy or high density aggregate are used to increase the density of concrete, and this is a very desirable property for the attenuation of photon radiation, and this results in a reduction of the thickness of the concrete required for radiation shielding. The specific gravity of ordinary aggregate for concrete lies between 2.5 and 3.0 g/cm³, whilst heavy aggregates have specific gravities exceeding 4.0 g/cm³, such as: Haematite (Fe₂O₃), Magnetite (Fe₃O₄), Ilmenite (FeO.TiO₂), Barytes (BaSO₄), Witherite (BaCO₃), and Ferrophosphorus (FeP, Fe₂P, or Fe₃P)

Boron-Containing Materials

The capture and attenuation of thermal neutrons usually results in the production of hard or penetrating gamma radiation. To reduce, or suppress, the production of this secondary-capture gamma radiation elements with very large absorption neutron cross-section can be used, resulting in the emission of soft gamma rays which are less penetrating and readily absorbed within a radiation shield. Boron has two stable isotopes, boron-10 and boron-11. The higher isotopes boron-10 has a very high absorption capacity for thermal neutrons, resulting in the emission of weak or soft capture gamma radiation which is easily absorbed by the shield, and hence boron is regarded as an effective element over others (such as hydrogen or silicon). Boron and boron compounds are often used in concrete to increase the probability of neutron capture without producing secondary capture gamma rays of high energy. The high

capture capability of boron-10 allows for the use of relatively small quantities in the concrete mixture, and 1% of boron by weight is generally considered to be adequate. Concrete is generally boronated by the incorporation of borate minerals or synthetic boron frits. Other methods are the use of ground pyrex glass, the use of boric acid or complex borates dissolved in the mixing water and the use of boron in the cementing agent. Commercial boron minerals are mainly consist of calcium, sodium and magnesium borate precipitate from waters in arid volcanic regions or alteration products of these precipitates such as:

Colemanite ($2\text{CaO} \cdot 3\text{B}_2\text{O}_3 \cdot 5\text{H}_2\text{O}$)
Borocalcite ($\text{CaO} \cdot 2\text{B}_2\text{O}_3 \cdot 4\text{H}_2\text{O}$)
Ulexite
Paigeite and
Tourmaline
Boron –frit Glasses
Boron Carbide of different composition (B_6C , B_4C or B_3C)
Ferroboron
Colemanite-baryes Frit

6- Design of Concrete for Radiation Shielding

Basic design of concrete for radiation shielding consists of the following steps:

- a- The type and intensity of the radiation source must be ascertained. In nuclear reactors for example, the type and design of the reactor will determine the type and intensity of the radiation to which the radiation shield will be expected.
- b- The maximum level of radiation that can be permitted at the external surface of the shield must be according to the issued regulations.
- c- The required attenuation coefficient or reduction factor must be ascertained.
- d- Consideration is given to the choice and proportioning of materials, which could be used in concrete to validate the physical and mechanical properties of concrete materials and concrete mixes.
- e- Estimating the thickness of the concrete required to achieve the required attenuation.
- f- The temperature distribution in the concrete shield is ascertained so that the thermal stress may be calculated to establish whether they are within acceptable limits.
- g- The cost of the manufacturing of concrete for radiation shielding.
- h- The method of selecting and adjusting mix proportions for normal weight or ordinary concrete to follow the published ACI 211.1-81.

7- Experimental Measurement of γ -ray Attenuation in Grancrete™ Concretes Product GCI 2000

7.1- Experimental Setup:

The experimental setup is shown in Figure 1 in which a radiation source is placed on the bottom base, collimated by lead collimators. The sample is placed on top of the collimators. The detector is placed inside a lead shield and the detection window is collimated by lead collimators. The detector is a 2" x 2" NaI(Tl) crystal with 5 - 7% energy resolution. This arrangement is known as *narrow-beam arrangement* that provides good geometry and better collimation. Measuring concrete attenuation of γ -ray is determined by measuring the fractional radiation intensity $I(x)$ passing through the thickness x as compared to the source intensity $I(o)$. The attenuation coefficient μ is obtained from the solution of the exponential law $I_x = I_o e^{-\mu x}$. This attenuation coefficient is compared to ordinary concrete for the various concrete mixes.

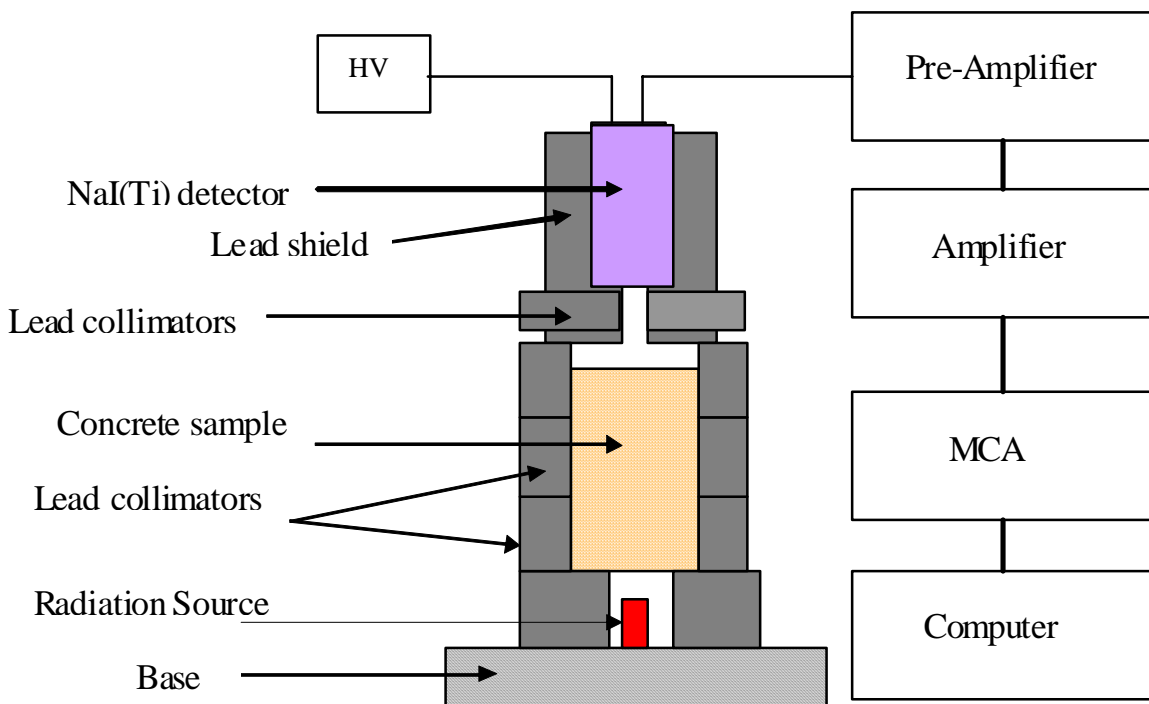


Figure 1 Experimental arrangement for measuring γ -ray attenuation in concrete samples

Two radiation sources are used to evaluate the attenuation coefficient of the concrete samples, a 1.0 μ Ci cobalt-60 (Co-60) at two photon energies of 1.173 and

1.332MeV, and a 5 μ Ci Cesium-137 (Cs-137) at photon energy of 0.662MeV. Table 1 shows the sources, their activity and the photon energies.

Table 1 Sources, their activity and their photon energies

Source	Activity (μ Ci)	Photon Energy (MeV)
Co-60	1.0	1.173
		1.332
Cs-137	5.0	0.662

Background radiation is measured prior to each experiment and all data are background-corrected. All measurements were taken for a fixed preset time for each sample and selection of a narrow region symmetrical with respect to the centroid of the photo peak (R. M. Mayo and D.E. Peplow, 2000).

The measurements were carried out on three different groups of Grancrete concrete product named samples group (A), samples 2nd group of group (A) and samples group (B). The physical and mechanical properties of these groups are listed in Appendix 1.

7.2- Experimental Results of Grancrete™ Groups A and B:

7.2.1- Test Results on the Attenuation of γ -Rays “Group A”

Table 2 lists the Grancrete concrete samples group (A) tested for attenuation. The table also shows the samples' mixture, measured thickness and calculated density. All samples are cast cylindrically and have same diameter of 4-inches, however, the thickness varies as shown in Table 2. Figure (2) shows the density of each sample as a percentage with respect to the ordinary concrete, where all samples density varies between 57-74.9% (except sample A10, which is 46.5%) of ordinary concrete.

A- Results using 5 μ Ci Cs-137 source, photon energy 0.662MeV:

The attenuation coefficient of the tested concrete mixes is shown in Figure 3. The measurements were carried out for 10min counting time for each sample. It is clear that sample A6, A4, and A5 has the highest attenuation coefficient ($\mu = 0.181, 0.178, \text{ and } 0.172 \text{ cm}^{-1}$), which are nearest to ordinary concrete ($\mu = 0.19 \text{ cm}^{-1}$). Sample A15, A16 and A2 is next in their attenuation performance ($\mu = 0.164, 0.164, 0.163 \text{ cm}^{-1}$), followed by samples A11, A17, A3 and A9 ($0.162, 0.159, 0.158, \text{ and } 0.158 \text{ cm}^{-1}$). This means that these samples have attenuation coefficient varies between 69.3-95.8 % of the value of ordinary concrete (OC). Sample A10 gives the lowest value, which is approximately 59.3% of ordinary concrete; this sample has the lowest density.

Table 2 Grancrete™ concrete samples Group A (Product GCI 2000) tested for γ -ray attenuation

Sample Number	Grancrete ID number	Sample Mixture	Thickness (inch)	Density gm/cm ³
1	A1	None	8.125	1.61
2	A2	Sand (2parts GC:1 part Sand)	8.05	1.76
3	A3	3/8" Pea gravel (2:1)	7.79	1.46
4	A4	1/2" Granite (2:1)	8.05	1.57
5	A5	1/2" Marble (2:1)	8.01	1.68
6	A6	1"+ Stone (2:1)	8.03	1.65
7	A7	Natural FeO (2%)	8.11	1.73
8	A8	Syn FeO 2%	8.06	1.39
9	A9	Granite gravel (2:1)	8.03	1.51
10	A10	Vermiculite (5:1)	8.06	1.09
11	A11	Slate Gravel (2:1)	8.08	1.64
12	A12	ShaleGravel (2:1)	8.04	1.51
13	A13	recycled Rubber (2:1)	8.05	1.36
14	A14	Wollastonite (20%)	8.00	1.41
15	A15	Boric Acid (1%)	8.06	1.49
16	A16	Borax (5%)	8.00	1.39
17	A17	Borax (1%)	8.03	1.38
18	A18	Poly vinyl fibers (2%)	8.06	1.34
19	A19	Shogun fibers (2%)	8.08	1.38
20	A20	Fiberglass fibers (2%)	8.08	1.42
21 (NCSU Reference)	ORC (NCSU Reference)	ORDINARY CONCRETE (Reference, by NCSU)	--	2.35 (Lamarsh & Baratta)

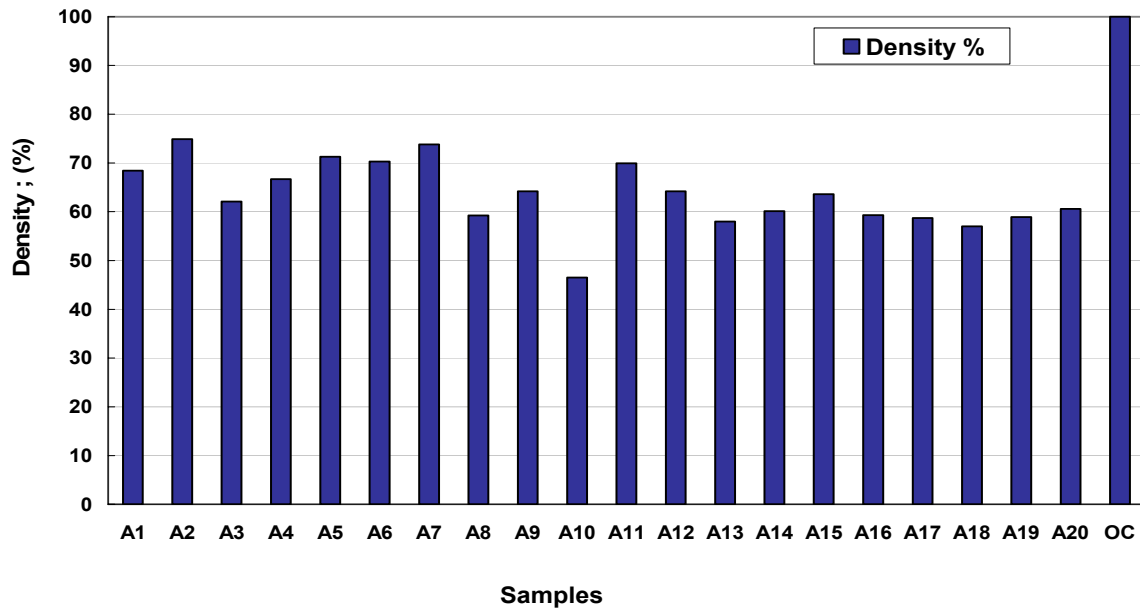


Figure 2 Density of samples as a percentage with respect to ordinary concrete

B- Results using 1 μ Ci Co-60 source, photon energy 1.173MeV:

The attenuation coefficient of the concrete mixes is shown in Figure 4. The measurements were carried out for 30min counting time for each sample. It is clear from the figure that sample A4, A9, and A14 have slightly higher value of attenuation coefficient ($\mu=0.136, 0.135$ and 0.134 cm^{-1}) than that of ordinary concrete ($\mu = 0.133 \text{ cm}^{-1}$). Samples A6, A3, A8, A2 and A16 follow them by values of ($\mu=0.131, 0.127, 0.126, 0.121$ and 0.12 cm^{-1}), which is about 98.3, 95.3, 94.6, .90.1, and 90.1% of that of ordinary concrete. It is also clear that sample A10 gives the lowest value as compared to ordinary concrete.

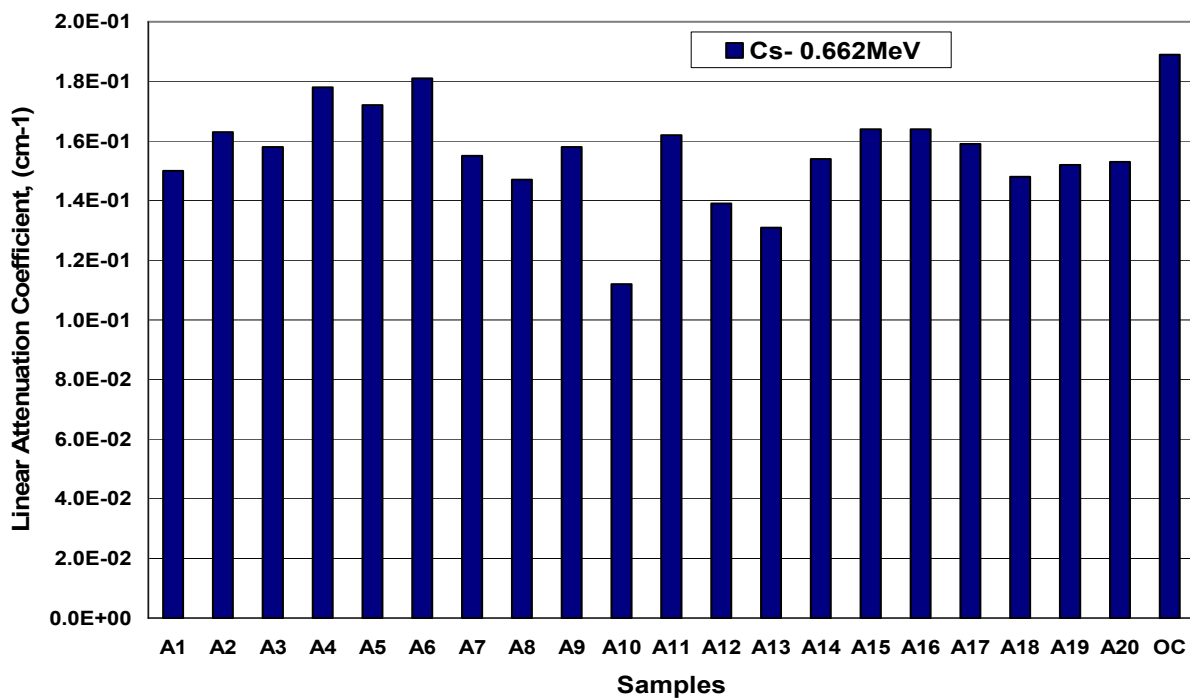


Figure 3 Attenuation coefficients of the various concrete mixes for 0.662MeV photon energy using a 5 μ Ci Cs-137 source

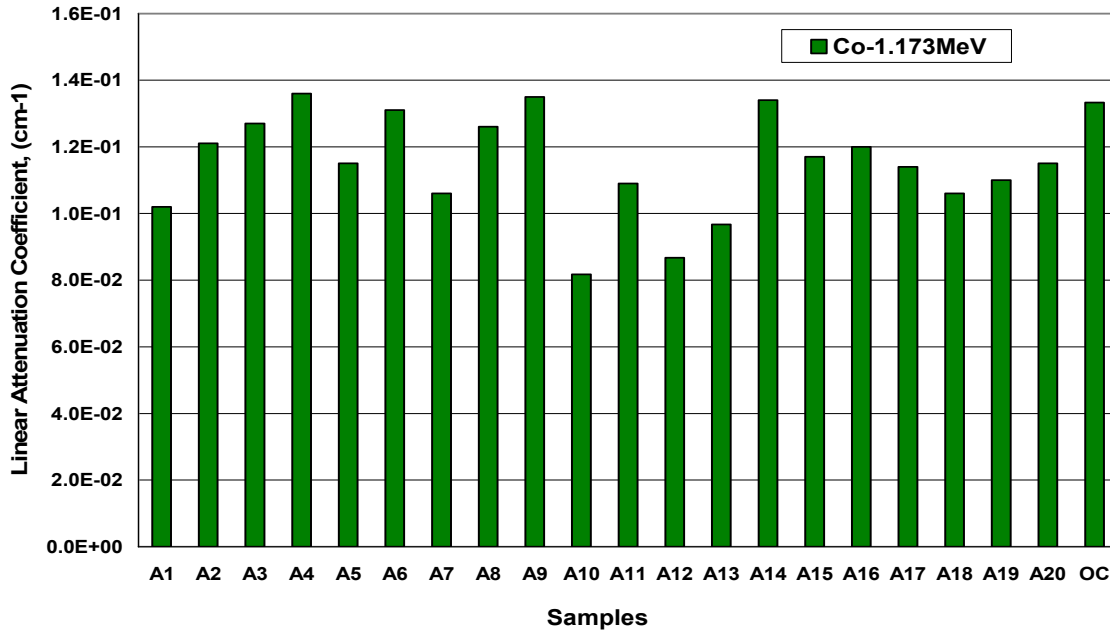


Figure 4 Attenuation coefficients of the various concrete mixes for photon energy of 1.173MeV using a 1 μ Ci Co-60 source

C- Results using 1 μ Ci Co-60 source, photon energy 1.332MeV:

The attenuation coefficient of the concrete mixes is shown in Figure 5. The measurements were carried out for 30min counting time for each sample. It is clear that the majority of samples have higher attenuation coefficient than the ordinary concrete at photon energy 1.332 MeV except samples A12 and A13 have approximately the same value of about 0.108, 0.11cm⁻¹ where the ordinary concrete is 0.1215cm⁻¹, and sample A10 ($\mu=0.0884\text{cm}^{-1}$) is less than ordinary concrete by about 27.2%. It is clear that sample A6 has the highest attenuation coefficient ($\mu=0.186\text{cm}^{-1}$) for the 1.332MeV (a factor of 1.53 better than ordinary concrete). Samples A4, A9 and A14 are next in their performance with attenuation coefficient of about $\mu=0.171$, 0.169 and 0.162 cm⁻¹, respectively; which is greater than that of ordinary concrete by a factor of 1.41, 1.39 and 1.33, respectively. Samples A3, A8 and A5 have attenuation coefficients of 0.159, 0.156 and 0.148, respectively; which are greater than that of ordinary concrete by a factor of about 1.31, 1.28 and 1.22, respectively.

Figure 6 shows the attenuation coefficient of all samples at the 3 photon energies of 0.662, 1.173 and 1.332MeV. It is to be recognized that the data for the 0.662 energy is for a 5 μ Ci source (Cs-137), which is a factor of 5 higher than that of the Co-60 (1 μ Ci), and hence the attenuation for the lower photon energy is attenuation of stronger source intensity but at lower photon energy. Figure 7 shows the compressive strength of samples group A after test (in Kg/cm²).

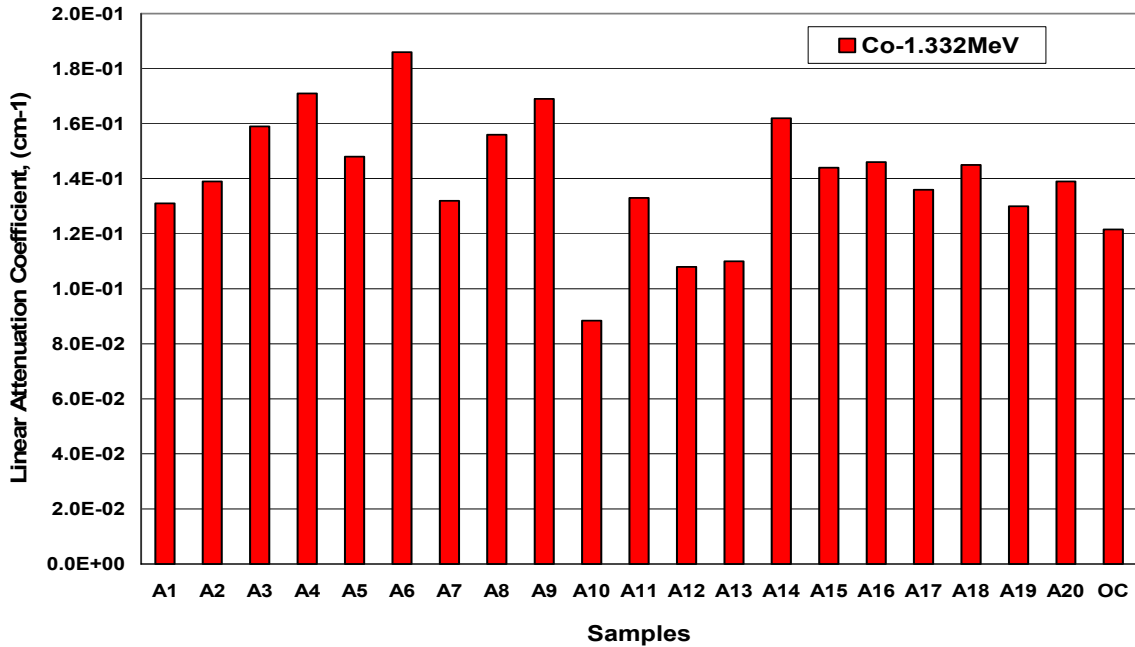


Figure 5 Attenuation coefficients of the various concrete mixes for photon energies of 1.332 MeV using a 1 μ Ci Co-60 source

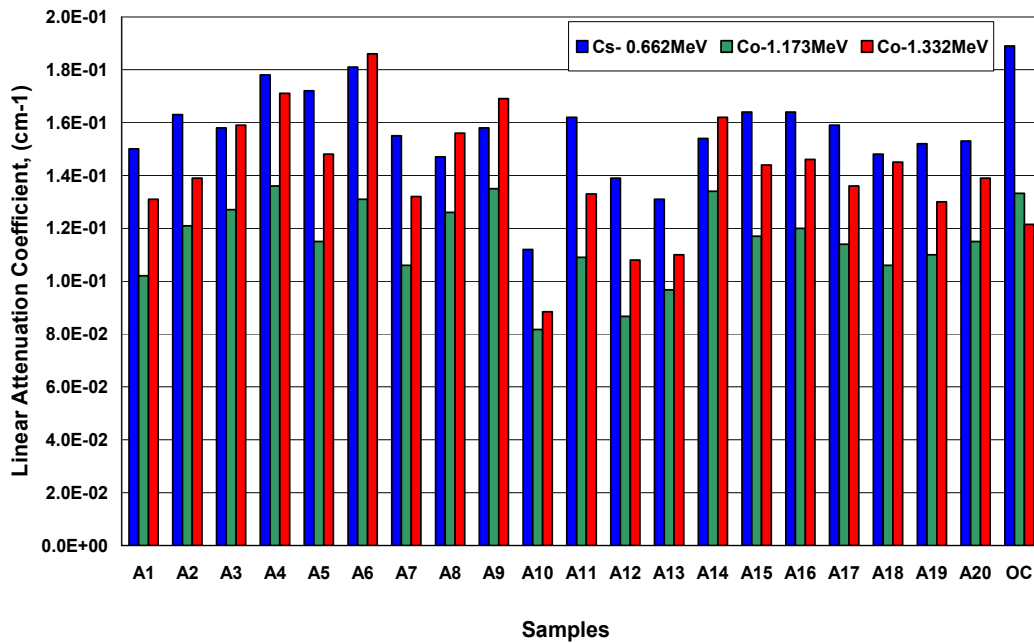


Figure 6 Attenuation coefficients of the various concrete mixes for photon energies of 0.662MeV (5 μ Ci Cs-137 source) and 1.173 and 1.332MeV (1 μ Ci Co-60 source).

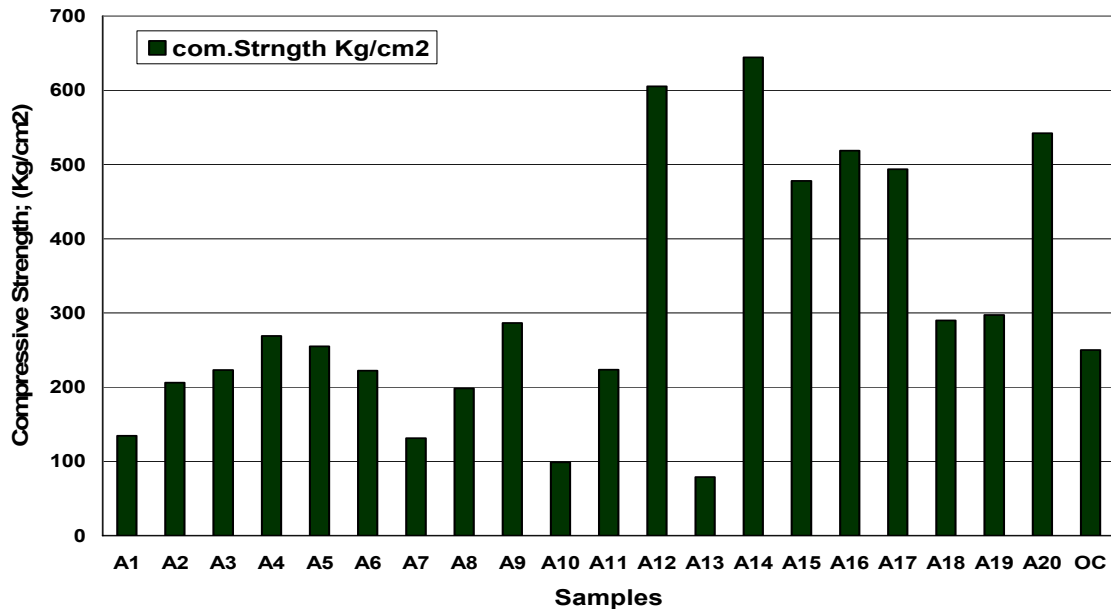


Figure 7 Compressive strength of samples group A after test

7.2.2 - Test Results on the Attenuation of γ -Rays “2nd Group A”

Table 3 lists the 2nd group of Grancrete concrete samples group (A) tested for attenuation. The table also shows the samples’ mixture, measured thickness and calculated density. All samples are cast cylindrically and have same diameter of 4-inches, however, the thickness varies as shown in Table 3. Figure (8) shows the density of each sample as a percentage with respect to the ordinary concrete, where all samples density varies between 55.9 -75.4% of ordinary concrete.

A- Results using 5 μ Ci Cs-137 source, photon energy 0.662MeV:

The attenuation coefficient of the tested concrete mixes is shown in Figure 9. The measurements were carried out for 10min counting time for each sample. It is clear that sample A5, A6, A3, A4, and A15 has the highest attenuation coefficient ($\mu = 0.178, 0.178, 0.177, 0.177, 0.170 \text{ cm}^{-1}$), which are nearest to ordinary concrete (OC) ($\mu = 0.19 \text{ cm}^{-1}$), i.e. of about 94.4, 94.0, 93.7, 93.5, and 90.1 % of ordinary concrete. Samples A8, A2, A9, and A10 are next in their attenuation performance ($\mu = 0.166, 0.166, 0.165$ and 0.162 cm^{-1}) which are about 87.9, 87.8, 87.2, 85.6% of ordinary concrete, followed by samples A1, A7, A11, A12, A14 and A13 ($0.157, 0.157, 0.154, 0.153, 0.150, 0.148 \text{ cm}^{-1}$) which varies between 83.3-78.2% of the value of ordinary concrete. Sample A13 gives the lowest attenuation coefficient value, which is approximately 78.2% of ordinary concrete, and has density of approximately 56.7% of ordinary concrete.

It is noted that this group samples have attenuation coefficient values vary between 78.2-94.4 % of the value of ordinary concrete with the photon energy of 0.662MeV, and their densities vary between 55.9 -75.4% of ordinary concrete.

Table 3 Grancrete™ concrete samples Group A (Product GCI 2000) tested for γ -ray attenuation

Sample Number	Grancrete ID number	Sample Mixture	Amount (%)	Thickness (cm)	Density gm/cm ³
1	A1	NONE	0	20.4	1.60
2	A2	GRANITE SAND	33	20.5	1.31
3	A3	GRANITE GRAVEL (0.25")	33	20.3	1.69
4	A4	GRANITE STONE (0.5")	33	20.3	1.77
5	A5	GRANITE STONE (1.0")	33	20.4	1.62
6	A6	PEA GRAVEL (0.25"-0.5")	33	20.4	1.61
7	A7	BORIC ACID	1	20.3	1.61
8	A8	BORAX	10	20.4	1.54
9	A9	BORAX	5	20.3	1.62
10	A10	WOLLASTONITE	20	20.3	1.48
11	A11	PPG FIBERGLASS 3075	2	20.5	1.32
12	A12	PPG FIBERGLASS CHOP	2	20.3	1.33
13	A13	PPG FIBERGLASS CHOP	2	20.5	1.33
14	A14	PPG WOVEN ROVEN	4 LAYERS	20.4	1.34
15	A15	LEAD GLASS CHIPS	33	20.4	1.48
16 (NCSU Reference)	ORC (NCSU Reference)	ORDINARY CONCRETE (Reference, by NCSU)	--	--	2.35 (Lamarsh & Baratta)

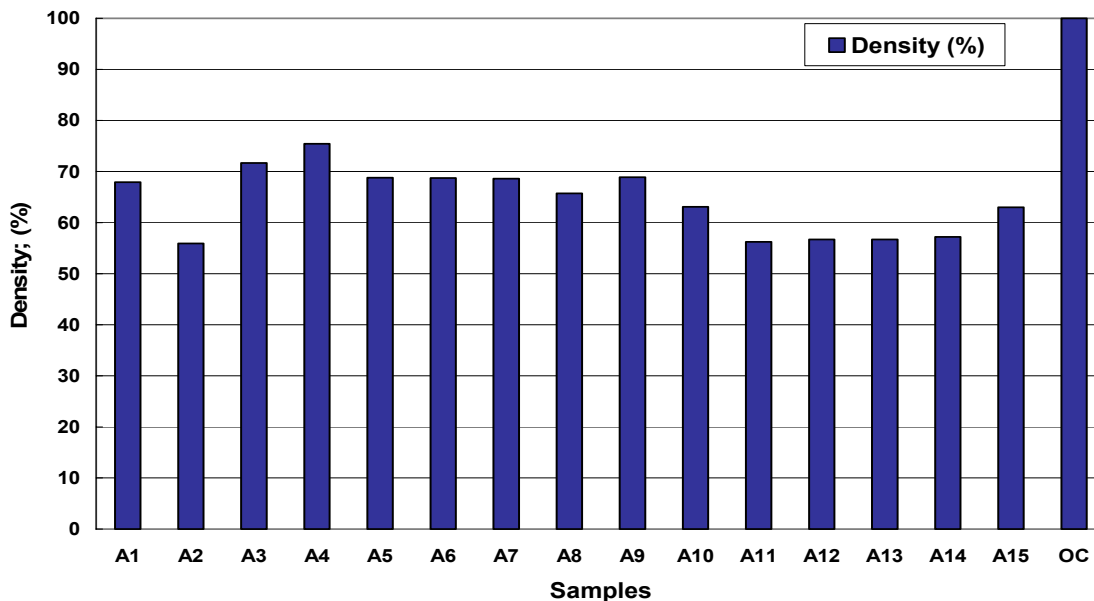


Figure 8 Density of samples as a percentage with respect to ordinary concrete

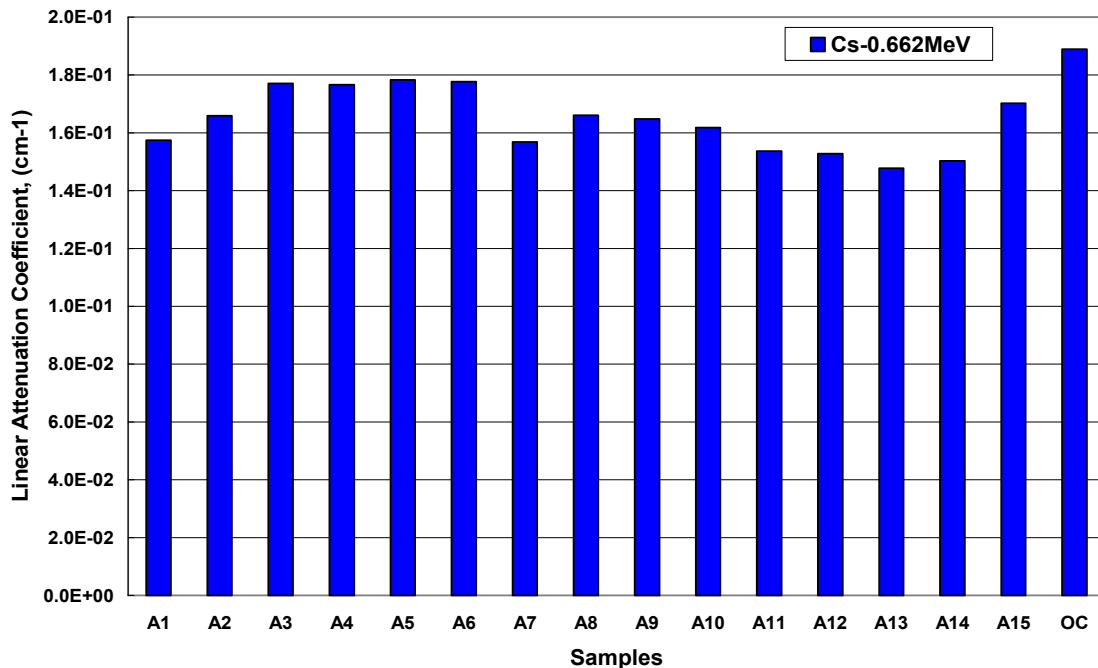


Figure 9 Attenuation coefficients of the various concrete mixes for 0.662MeV photon energy using a 5mCi Cs-137 source

B- Results using 1 μ Ci Co-60 source, photon energy 1.173MeV:

The attenuation coefficient of the concrete mixes is shown in Figure 10. The measurements were carried out for 30min counting time for each sample. It is clear from the figure that sample A6 have slightly higher value of attenuation coefficient ($\mu=0.141 \text{ cm}^{-1}$) reach to 105% than that of ordinary concrete ($\mu = 0.133 \text{ cm}^{-1}$). Samples A5, A3 and A4, follow A6 by values approximately equal to the attenuation coefficient of ordinary concrete of ($\mu=0.134, 0.133$ and 0.132 cm^{-1}), which is about 100.0, 99.5, 99.0, % of that of ordinary concrete. Samples A2 , A15, A10, and A7 have attenuation coefficient of about ($\mu=0.128, 0.124, 0.123$ and 0.121 cm^{-1}) which are less than the value of ordinary concrete by about 3.8, 7.2, 7.4, 9.5% respectively. Samples A9, A11, A12, A14, A1, A8, A13 have attenuation coefficient of about ($\mu=0.119, 0.116, 0.115, 0.114, 0.114, 0.11$ and 0.0995 cm^{-1}) which are 89, 86.9, 86.3, 85.6, 85.5, 82.9, and 74.7% of ordinary concrete respectively.

It is also clear that sample A6 and A13 with attenuation coefficient values reach to 105% and 74.7% give the highest and lowest value of ordinary concrete.

It is noted that this group samples have attenuation coefficient values vary between 74.7- 105 % of the value of ordinary concrete with the photon energy of 1.173 MeV.

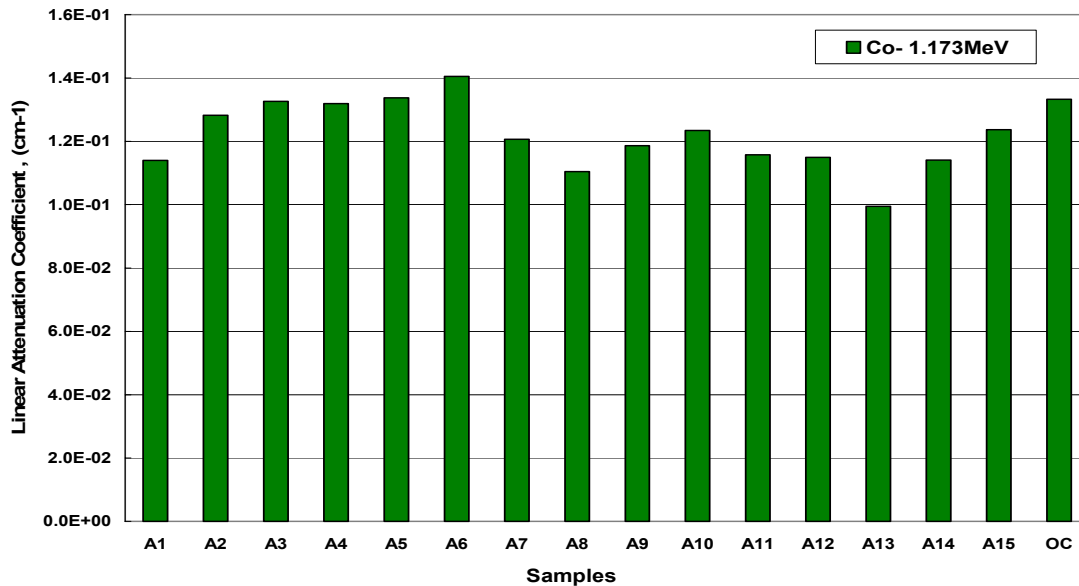


Figure 10 Attenuation coefficients of the various concrete mixes for photon energy of 1.173MeV using a 1 μ Ci Co-60 source

C- Results using 1 μ Ci Co-60 source, photon energy 1.332MeV:

The attenuation coefficient of the concrete mixes is shown in Figure 11. The measurements were carried out for 30min counting time for each sample. It is clear that all the samples have higher attenuation coefficient than the ordinary concrete (0.1215cm^{-1}) at photon energy 1.332 MeV, and their values varies between 118 and 155%, except sample A13 have slightly value about 103%. It is clear that sample A5 has the highest attenuation coefficient ($\mu=0.189\text{cm}^{-1}$), i.e. a factor of 1.55 better than ordinary concrete. Samples A4, A6, A3, A15 and A2 are next in their performance with attenuation coefficient of about ($\mu=0.181, 0.176, 0.169, 0.162$ and 0.158cm^{-1}), respectively; which is greater than that of ordinary concrete by a factor of 1.49, 1.45, 1.39, 1.33 and 1.30 respectively. Samples A7, A9, A11, A10, A12, A14, A8 and A13 have attenuation coefficients of 0.154, 0.154, 0.150, 0.148, 0.147, 0.144, 0.143, and 0.125cm^{-1} respectively; these values are greater than that of ordinary concrete by a factor of about 1.27, 1.27 and 1.23, 1.22, 1.21, 0.118, 0.118 and 1.03 respectively.

It is noted that these group samples have attenuation coefficient value higher than the value of ordinary concrete with the photon energy of 1.332 MeV.

Figure 12 shows the attenuation coefficient of all samples at the 3 photon energies of 0.662, 1.173 and 1.332MeV. It is to be recognized that the data for the 0.662 energy is for a 5 μ Ci source (Cs-137), which is a factor of 5 higher than that of the

Co-60 (1 μ Ci), and hence the attenuation for the lower photon energy is attenuation of stronger source intensity but at lower photon energy.

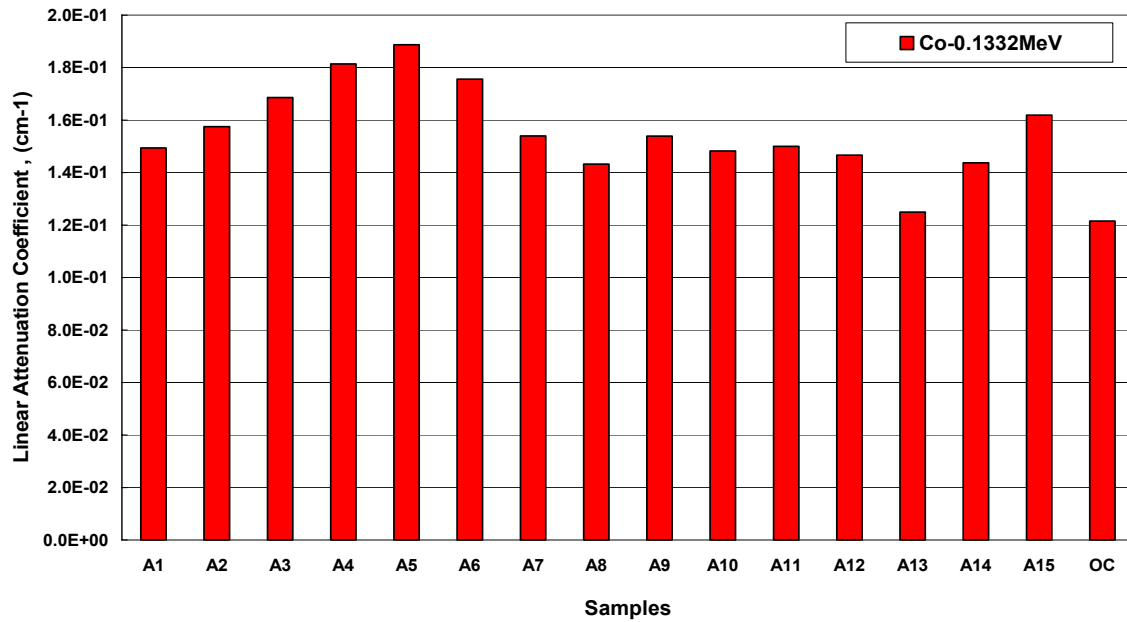


Figure 11 Attenuation coefficients of the various concrete mixes for photon energies of 1.332 MeV using a 1 μ Ci Co-60 source

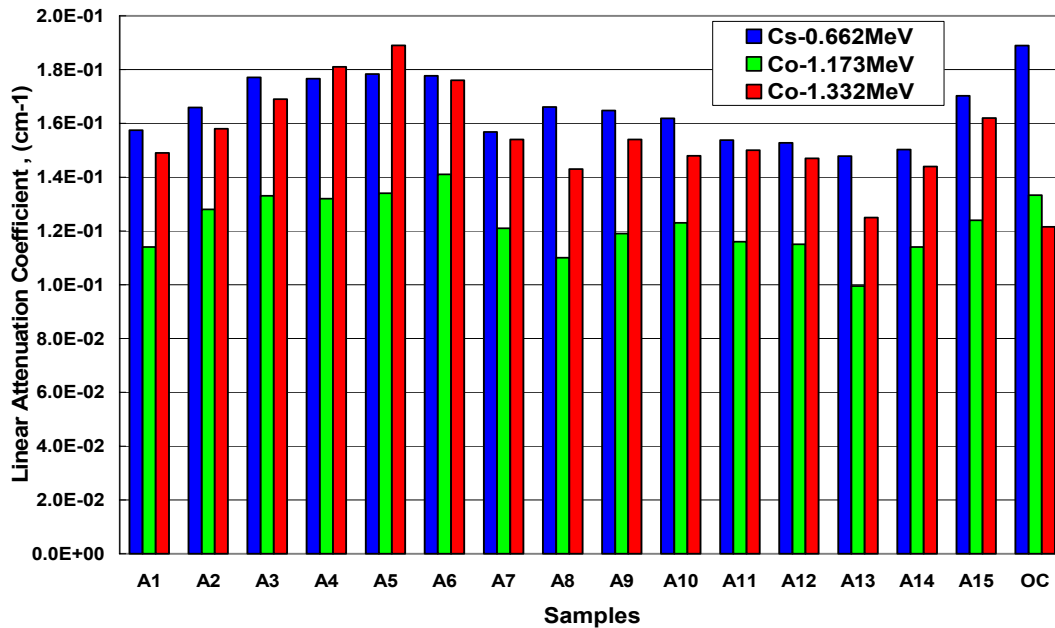


Figure 12 Attenuation coefficients of the various concrete mixes for photon energies of 0.662MeV (5 μ Ci Cs-137 source) and 1.173 and 1.332MeV (1 μ Ci Co-60 source).

Table 4 summarizes the density percent and linear attenuation coefficient percent of 2nd group of Grancrete™ concrete samples Group A (Product GCI 2000) as compared to ordinary concrete tested at 3 photon energies of γ -ray radiation of 0.662, 1.173 and 1.332MeV. Calculation of the mass attenuation coefficient (μ/ρ) cm^2g^{-1} may be obtained by dividing the attenuation coefficient by the specific density of each sample. For detailed computational evaluation, the exact composition of each sample would be need. Figure 13 shows the compressive strength of samples 2nd group A after test (in Kg/cm^2).

Table 4 Summary of the density percent and linear attenuation coefficient percent of 2nd group of Grancrete™ concrete samples Group A (Product GCI 2000) with respect to ordinary concrete tested at 3 photon energies of γ -ray radiation.

Sample Number	Grancrete ID number	Density (%)	Cs-137 0.662MeV (%)	Co-60 1.173MeV (%)	Co-60 1.332MeV (%)
1	A1	67.9	83.3	85.5	123.0
2	A2	55.9	87.8	96.2	130.0
3	A3	71.7	93.7	99.5	139.0
4	A4	75.4	93.5	99.0	149.0
5	A5	68.8	94.4	100.0	155.0
6	A6	68.7	94.0	105.0	145.0
7	A7	68.6	83.0	90.5	127.0
8	A8	65.7	87.9	82.9	118.0
9	A9	68.9	87.2	89.0	127.0
10	A10	63.1	85.6	92.6	118.0
11	A11	56.2	81.4	86.9	127.0
12	A12	56.7	80.9	86.3	122.0
13	A13	56.7	78.2	74.7	123.0
14	A14	57.2	79.5	85.6	121.0
15	A15	63	90.1	92.8	103.0
16 (NCSU Reference)	ORC (NCSU Reference)	100	100	100	100

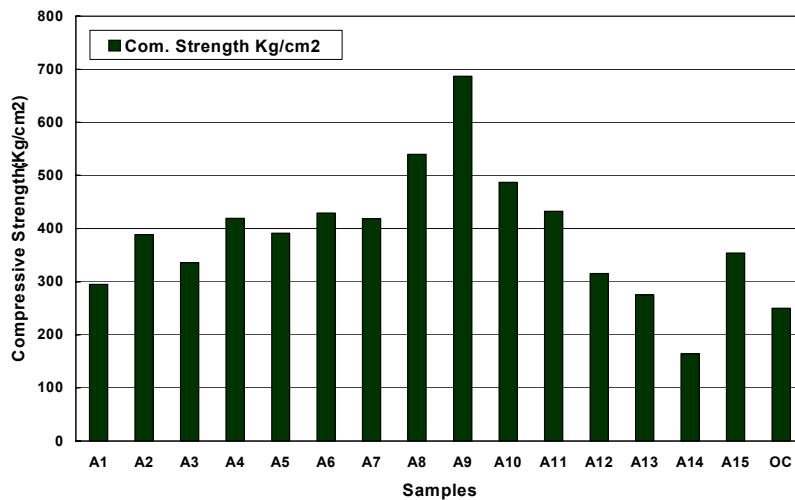


Figure 13 Compressive Strength of 2nd group of samples group A after test

7.2.3. Test Results on the Attenuation of γ -Rays “Group B”

Table 5 lists the Grancrete™ concrete samples group (B) tested for γ -ray attenuation. The table also shows the samples' mixture, measured thickness and calculated density. All samples are cast cylindrically and have same diameter of 4-inches, however, the thickness varies as shown in Table 5. Figure (14) shows the density of each sample as a percentage with respect to the ordinary concrete (OC), where all samples density varies between 64.0 - 81.7 % of ordinary concrete.

Table 5 Grancrete™ concrete samples Group B (Product GCI 2000) tested for γ -ray attenuation

Sample Number	Grancrete ID number	Added Material	Amount (%wt)	Thickness (cm)	Density gm/cm ³
1	B1	NONE	0	20.5	1.64
2	B2	GRANITE SAND	33	20.47	1.73
3	B3	GRANITE GRAVEL (0.25")	33	20.5	1.92
4	B4	GRANITE STONE (0.5")	33	20.42	1.65
5	B5	GRANITE STONE (1.0")	33	20.53	1.771
6	B6	PEA GRAVEL (0.25"-0.5")	33	20.5	1.773
7	B7	BORIC ACID	2	21.13	1.673
8	B8	BORAX	12	20.27	1.552
9	B9	BORAX	6	20.47	1.5
10	B10	METAKAOLIN	20	20.3	1.63
11	B11	PPG FIBERGLASS 3075	2	20.7	1.6
12	B12	PPG FIBERGLASS	2	20.5	1.59
13	B13	PPG FIBERGLASS	2	20.6	1.71
14	B14	LEAD GLASS CHIPS	33	20.47	1.81
15	B15	BORAX	3	20.3	1.68
16	B16	WOLLASTONITE	20	20.37	1.65
17	B17	LEAD SHOT	20	20.6	1.911
18 (NCSU Reference)	ORC (NCSU Reference)	ORDINARY CONCRETE (Reference, by NCSU)		--	2.35 (Lamarsh & Baratta)

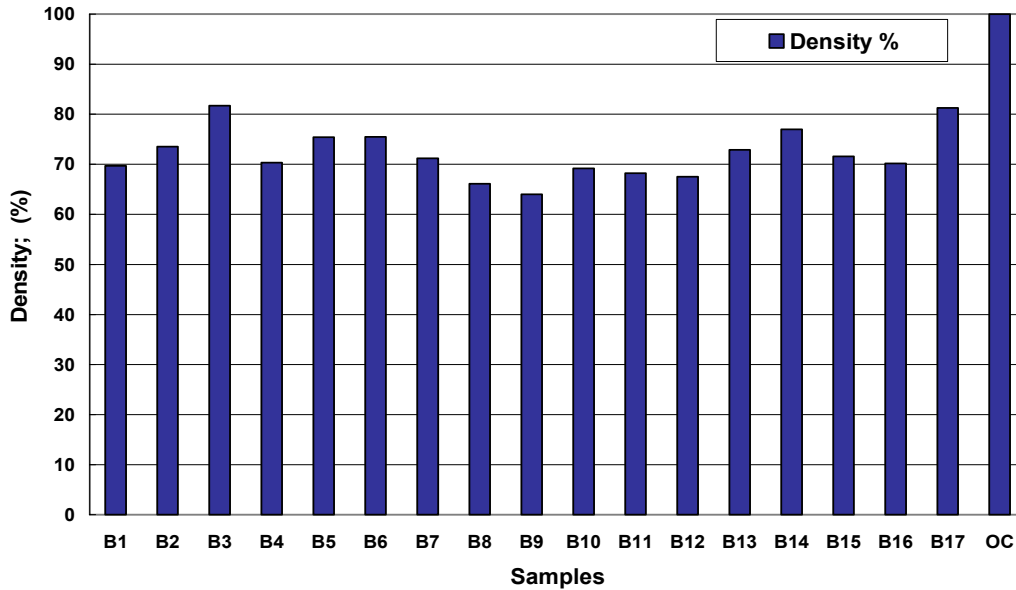


Figure 14 Density of samples as a percentage with respect to ordinary concrete

A- Results using 5 μ Ci Cs-137 source, photon energy 0.662MeV:

The attenuation coefficient of the tested concrete mixes is shown in Figure 15. The measurements were carried out for 10min counting time for each sample. Each test was repeated 3 times to obtain good averaging. It is clear that sample B17 has the highest attenuation coefficient ($\mu = 0.196\text{cm}^{-1}$), which is about 103.8% of the ordinary concrete (OC) ($\mu = 0.19\text{ cm}^{-1}$). The figure shows that B14, B6, and B3 have attenuation coefficient ($\mu = 0.187, 0.182, \text{ and } 0.181\text{ cm}^{-1}$), which are nearest to ordinary concrete (OC), i.e. of about 99.0, 96.1, and 95.6%, of ordinary concrete. Samples B5, B4, B2, B15, B9, and B1 are next in their attenuation performance ($\mu = 0.173, 0.171, 0.166, 0.164, 0.163 \text{ and } 0.162\text{ cm}^{-1}$) which are about 91.5, 90.4, 87.6, 86.8, 86.5, and 85.6 % of ordinary concrete, followed by samples B8, B12, B11, B16, B13, and B7 (0.160, 0.160, 0.158, 0.157, and 0.155, and 0.149 cm^{-1}) which varies between 81.9 to 84.9 % of the value of ordinary concrete. Sample B10 gives the lowest attenuation coefficient value of about 0.149 cm^{-1} (78.9%) of ordinary concrete, and has density of approximately 69.2% of ordinary concrete.

It is noted that this group of samples has attenuation coefficient values vary between 78.9-103.8 % of the value of ordinary concrete with the photon energy of 0.662MeV, and their densities vary between 64.0 to 81.7% of ordinary concrete.

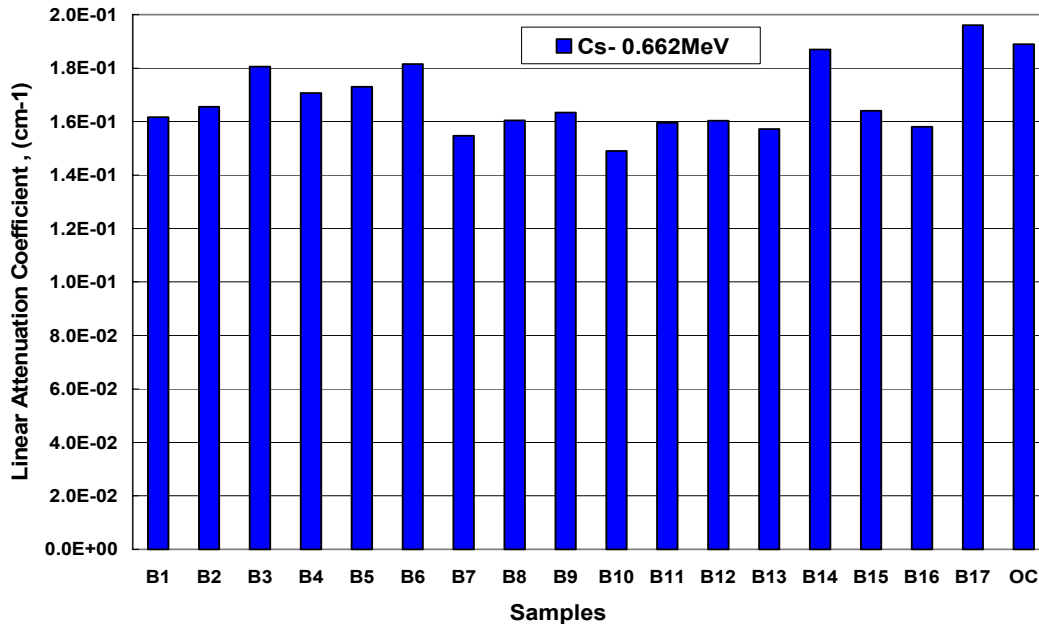


Figure 15 Attenuation coefficients of the various concrete mixes for 0.662MeV photon energy using a 5mCi Cs-137 source

B- Results using 1 μ Ci Co-60 source, photon energy 1.173MeV:

The attenuation coefficient of the concrete mixes is shown in Figure 16. The measurements were carried out for 30min counting time for each sample. Each test was repeated 3 times to obtain good averaging. It is clear from the figure that sample B6, B4, B17, and B3 have higher value of attenuation coefficient ($\mu=0.137, 0.136, 0.1357, 0.1355 \text{ cm}^{-1}$) reach to 102.7, 102.3, 101.9, and 101.7% than that of ordinary concrete ($\mu = 0.133 \text{ cm}^{-1}$). Samples B14, B5, B13 and B2, have values approximately equal to the attenuation coefficient of ordinary concrete of ($\mu=0.133, 0.132, 0.13$ and 0.127 cm^{-1}), which is about 99.8, 99.1, 97.3, 95.1% of that of ordinary concrete. Samples B11, B10, B15, B9, B1 and B16 have attenuation coefficient of about ($\mu=0.125, 0.1247, 0.124, 0.1227, 0.1226$ and 0.122 cm^{-1}) which are less than the value of ordinary concrete by about 6.2, 6.4, 6.8, 7.9, and 8.0% respectively. Samples B12, B8, B7, have attenuation coefficient of about ($\mu=0.114, 0.111, \text{ and } 0.109, \text{ cm}^{-1}$) which are 85.5, 83.2, and 82.2% of ordinary concrete, respectively.

It is also clear that sample B6 and B7 with attenuation coefficient values of 102.7% and 82.2% give the highest and lowest value of ordinary concrete.

It is noted that this group of samples have attenuation coefficient values vary between 82.2- 102.7 % of the value of ordinary concrete with the photon energy of 1.173 MeV.

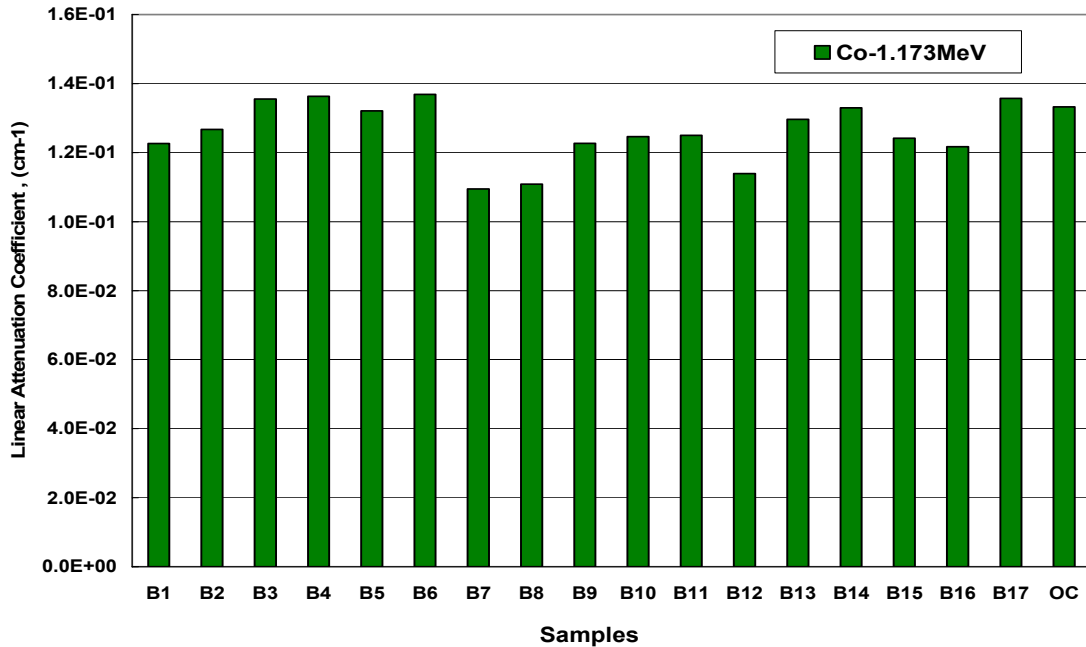


Figure 16 Attenuation coefficients of the various concrete mixes for photon energy of 1.173MeV using a 1 μ Ci Co-60 source

C- Results using 1 μ Ci Co-60 source, photon energy 1.332MeV:

The attenuation coefficient of the concrete mixes is shown in Figure 17. The measurements were carried out for 30min counting time for each sample. Each test was repeated 3 times to obtain good averaging. It is clear that all the samples have higher attenuation coefficient than the ordinary concrete (0.1215cm^{-1}) at photon energy 1.332 MeV and their values varies between 121.6 and 181.1%. It is clear that sample B17 has the highest attenuation coefficient ($\mu=0.220\text{cm}^{-1}$), i.e. a factor of 1.81 better than ordinary concrete. Samples B14, B5, B4, B3 and B6 are next in their performance with attenuation coefficient of about ($\mu=0.189, 0.1885, .18846, 0.1853, \text{ and } 0.177\text{cm}^{-1}$), respectively; which is greater than that of ordinary concrete by a factor of 1.55, 1.55, 1.55, 1.53, and 1.46 respectively. Samples B11, B1, B15, B9, B13, B16, B7 and B12 have attenuation coefficients of 0.168, 0.167, 0.164, 0.162, 0.161, 0.156, 0.153, and 0.153cm^{-1} respectively; these values are greater than that of ordinary concrete by a factor of about 1.39, 1.38, 1.35, 1.33, 1.32, 1.28, 1.26, and 1.25 respectively.

It is clear that all these group samples have attenuation coefficient value higher than the value of ordinary concrete at the photon energy of 1.332 MeV.

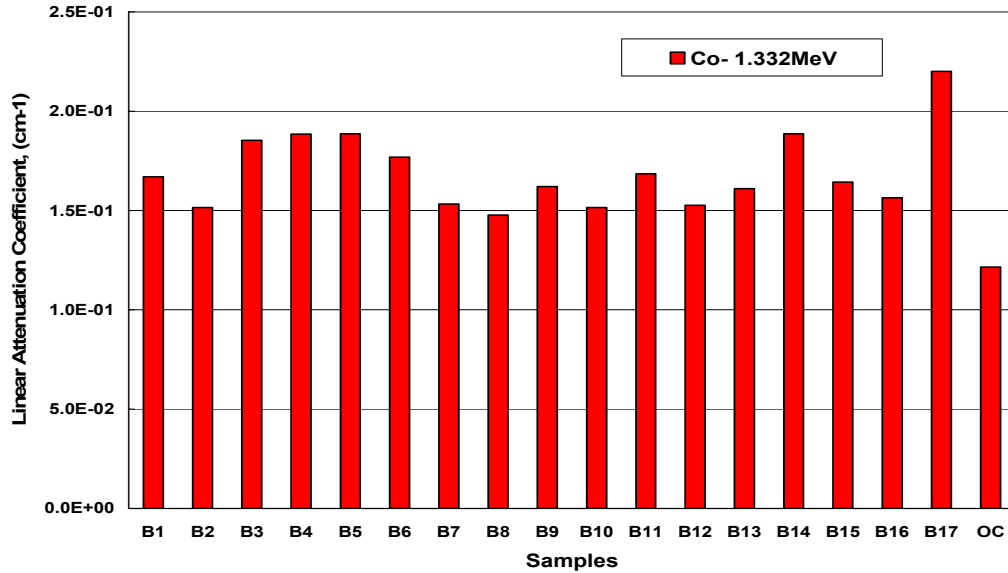


Figure 17 Attenuation coefficients of the various concrete mixes for photon energies of 1.332 MeV using a 1 μ Ci Co-60 source

Figure 18 shows the attenuation coefficient of all samples at the 3 photon energies of 0.662, 1.173 and 1.332MeV. It is to be recognized that the data for the 0.662 energy is for a 5 μ Ci source (Cs-137), which is a factor of 5 higher than that of the Co-60 (1 μ Ci), and hence the attenuation for the lower photon energy is attenuation of stronger source intensity but at lower photon energy.

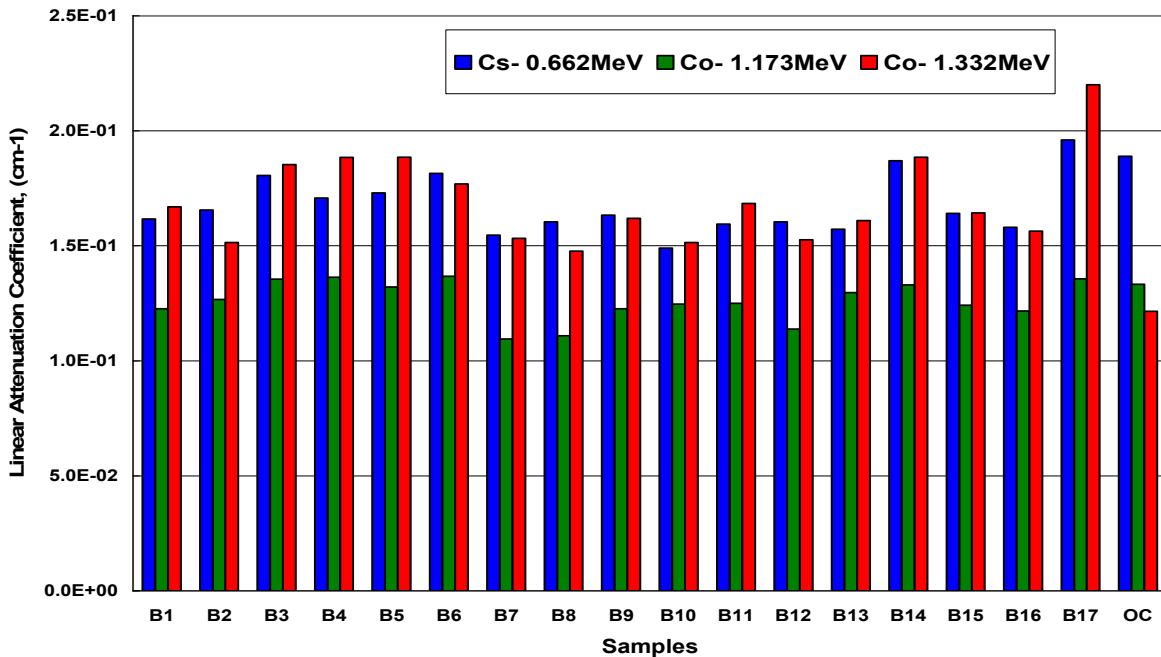


Figure 18 Attenuation coefficients of the various concrete mixes for photon energies of 0.662MeV (5 μ Ci Cs-137 source) and 1.173 and 1.332MeV (1 μ Ci Co-60 source).

Table 6 summarizes the density percent and linear attenuation coefficient percent of Grancrete™ concrete samples Group B (Product GCI 2000) as compared to ordinary concrete tested at 3 photon energies of γ -ray radiation of 0.662, 1.173 and 1.332MeV. Figure 19 shows the compressive strength of 2nd group of samples group A after test (in Kg/cm²).

Table 6 Summary of the density percent and linear attenuation coefficient percent of Grancrete™ concrete samples Group B (Product GCI 2000) with respect to ordinary concrete tested at 3 photon energies of γ -ray radiation.

Sample Number	Grancrete ID number	Density (%)	Cs-137 0.662MeV (%)	Co-60 1.173MeV (%)	Co-60 1.332MeV (%)
1	B1	69.7	85.6	92.0	137.5
2	B2	73.5	87.6	95.1	124.6
3	B3	81.7	95.6	101.7	152.5
4	B4	70.3	90.4	102.3	155.1
5	B5	75.4	91.5	99.1	155.2
6	B6	75.5	96.1	102.7	145.6
7	B7	71.2	81.9	82.2	126.2
8	B8	66.1	84.9	83.2	121.6
9	B9	64.0	86.5	92.1	133.3
10	B10	69.2	78.9	93.6	124.7
11	B11	68.2	84.4	93.8	138.7
12	B12	67.5	84.9	85.5	125.6
13	B13	72.9	83.2	97.3	132.5
14	B14	77.0	99.0	99.8	155.2
15	B15	71.6	86.8	93.2	135.2
16	B16	70.2	83.7	91.4	128.8
17	B17	81.3	103.8	101.9	181.1
16 (NCSU Reference)	ORC (NCSU Reference)	100	100	100	100

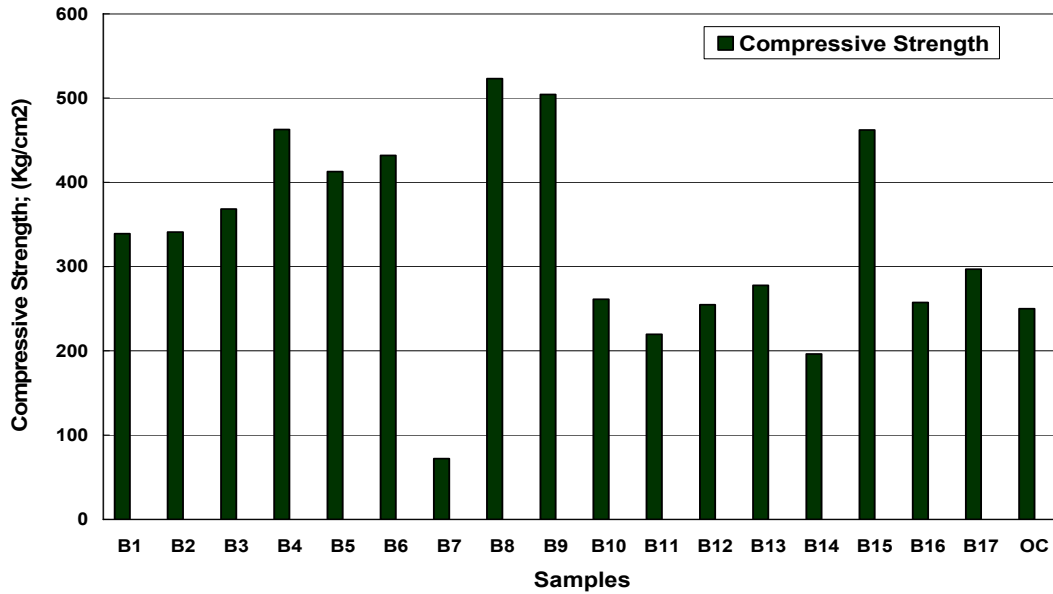


Figure 19 Compressive Strength of samples group B after test

8. Remarks on Grancrete™ Groups A and B results:

8.1. Remarks for 1st group of group (A)

Samples A4, A6, A9 and A14 are, in general, of better attenuation coefficient as compared to ordinary concrete. It is suggested to optimize the mixture of these samples to obtain most efficient results.

8.2. Remarks for 2nd group of group (A)

- 1- At photon energy of 0.662MeV, samples A5, A6, A3, A4 and A15 have attenuation coefficient values vary between 94.4-90.1 % of the value of ordinary concrete.
- 2- At photon energy of 1.173 MeV, samples A6, A5, A3, A4 and A2 have attenuation coefficient values vary between 105- 96.2 % of the value of ordinary concrete.
- 3- At photon energy of 1.173 MeV, all the samples have attenuation coefficient value higher than the value of ordinary concrete, and samples A5, A4, A6, A3 and A15 are the best of them.
- 4- In general samples A5, A4, A6, A3 and A15 are of better attenuation coefficient as compared to ordinary concrete and the other samples.

It is suggested to optimize the mixture of these samples for best optimal results.

8.3. Remarks for group (B)

- 1- At photon energy of 0.662MeV, sample B17 has a better attenuation coefficient than that of ordinary concrete (OC) by about 3.8%. Samples B3, B6, and B14, have attenuation coefficient values vary between 95.6-99.0 % of the value of ordinary concrete.
- 2- At photon energy of 1.173 MeV, samples B6, B4, and B17 and B3 have attenuation coefficients higher than that of ordinary concrete by about 2.7, 2.3, 1.9 and 1.7%, respectively. Samples B14, B5, B13, and B2 have attenuation coefficient values vary between 95.1 -99.0 % of the value of ordinary concrete.
- 3- At photon energy of 1.332 MeV, all samples have attenuation coefficients higher than the value of ordinary concrete. Sample B17 gives the highest one by a factor of about 1.81 % of ordinary concrete. Samples B14, B5, B4, and B3 have attenuation coefficient values bigger by a factor over 1.5 of the ordinary concrete.
- 2- In general samples B17, B14, B6, B5, B4, B3, are of better attenuation coefficient as compared to ordinary concrete, and as compared to all the other samples.
It is suggested to optimize the mixture of these samples for optimal best results.

Calculation of the mass attenuation coefficient (μ/ρ) cm^2g^{-1} may be obtained by dividing the attenuation coefficient by the specific density of each sample. For detailed computational evaluation, the exact composition of each sample would be need.

9. Test Results on the Attenuation of γ -Rays Composed HFR Samples

9.1 Experimental Setup

The experimental setup, as shown in Figure 20, is a standard radiation detection system. A radiation source is placed on the bottom base and is collimated by lead collimators. The sample is placed on top of the source collimator and the detector is placed inside a lead shield and the detection window is collimated by lead collimators. The radiation source is a stacked 5 sources $1\mu\text{Ci}$ each, 2 are Cs-137 and 3 are Co-60. The detector is an ORTEC Sodium Iodide (NaI(Tl)) 2" x 2" crystal Model 905-3 with photomultiplier tube base Model 226, with 5 - 7% energy resolution. The detector is powered by an ORTEC high voltage power supply Model 456 (0-3kV). The detector output is connected to an ORTEC amplifier Model 485 and the amplifier output is fed to

the multichannel analyzer (MCA), with is installed inside a computer. The computer is a Dell PC Optiplex 755 with the MCA card and software installed (CANBERRA Genie 2000). The Canberra Genie 2000 Gamma Acquisition and Analysis is used as the software platform for the transmitted gamma spectroscopy acquisition. Genie 2000 is a comprehensive set of capabilities for acquiring and analyzing spectra from Multichannel Analyzers. Its functions include MCA control, spectral display and manipulation, basic spectrum analysis and reporting.

Figure 21 illustrates the stacked sources, where the assembly is composed of 2 Cs-137 sources emitting γ -ray at photon energy of 0.662MeV, and 3 Co-60 sources emitting γ -ray at 2 photon energies of 1.173 and 1.332MeV, and Table 1 lists the sources, their activity and their photon energies. This arrangement allows for counting of the all photon peaks simultaneously without replacing the sources. Figure 22 is a pictorial illustration of the experimental setup.

Measuring concrete attenuation of γ -ray is determined by measuring the fractional radiation intensity $I(x)$ passing through the thickness x (the cylinder length for the cylindrical samples) as compared to the source intensity $I(o)$. The attenuation coefficient μ is obtained form the solution of the exponential law $I_x = I_o e^{-\mu x}$. This attenuation coefficient is compared to ordinary concrete for the various concrete mixes. The entire arrangement represents the standard technique for radiation detection and measurement of γ -ray attenuation in materials.

List of Instrumentation:

- Radiation source: Stacked 5 sources, 2 Cs-137 and 3 Co-60, each source is $1\mu\text{Ci}$ activity, as indicated in Table 7
- Detector: ORTEC Sodium Iodide NaI(Tl) Detector Model 905-3, 2"×2" with Photomultiplier Tube base (Model 266)
- Amplifier: ORTEC Model 485
- High Voltage Power Supply: ORTEC Model 456 (0-3kV)
- Computer with MCA: Dell PC Optiplex 755 with MCA card and software: Canberra Genie 2000. The Canberra Genie 2000 Gamma Acquisition & Analysis was used as the software platform for the transmitted gamma spectroscopy acquisition. Genie 2000 is a comprehensive set of capabilities for acquiring and analyzing spectra from Multichannel Analyzers (MCAs).Its functions include MCA control, spectral display and manipulation, basic spectrum analysis and reporting. Background radiation is measured prior to each experiment and all data are background-corrected.

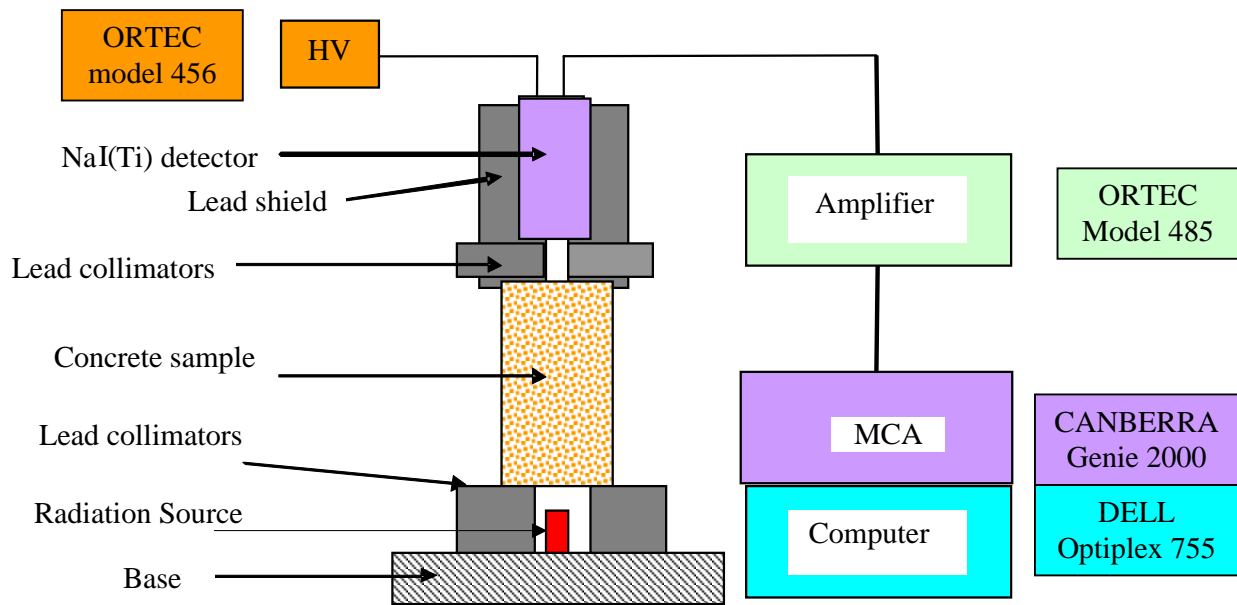


Figure 20 Experimental arrangement for measuring γ -ray attenuation in Grancrete™ cylindrical concrete samples, model of each instrument is also indicated

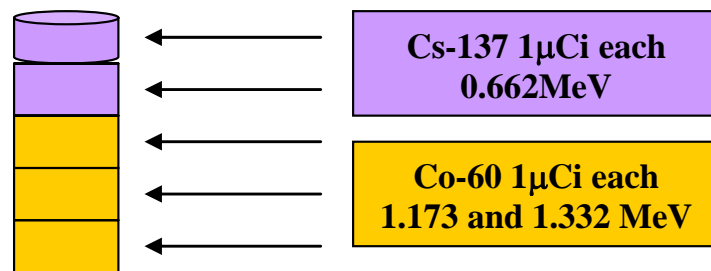


Figure 21 Radiation Source arrangement for simultaneous γ -ray attenuation measurements in cylindrical Grancrete samples

Table 7 Sources, their activity and their photon energies

Source	Activity (μ Ci)	Number of sources	Photon Energy (MeV)
Co-60	1.0	3	1.173 1.332
Cs-137	1.0	2	0.662

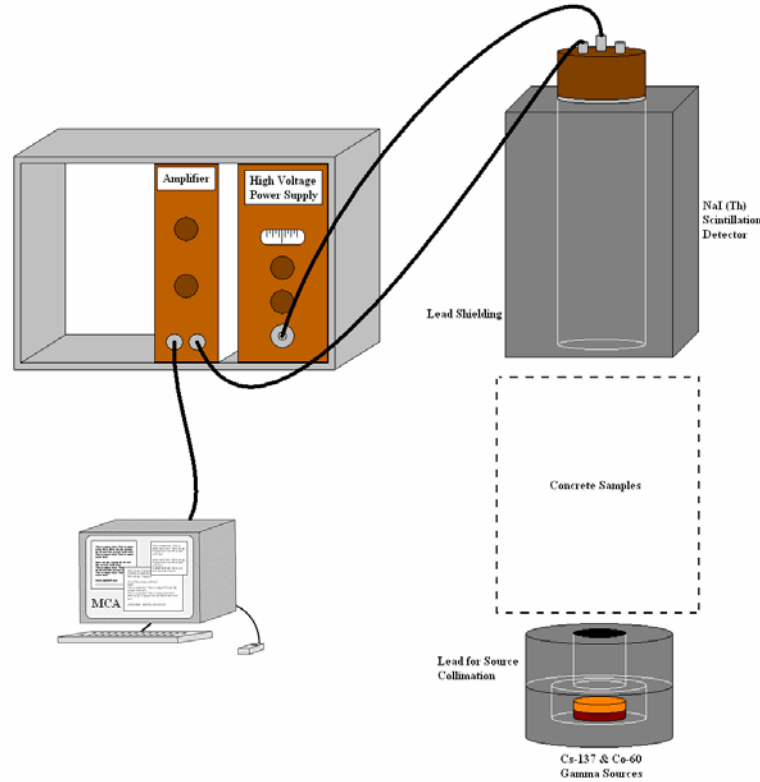


Figure 22 Illustration of the experimental arrangement for measuring γ -ray attenuation in Grancrete™ HFR cylindrical samples

9.2 Grancrete™ HFR Samples:

Table 8 lists the Grancrete™ HFR cylindrical concrete samples tested for γ -ray attenuation. The table also shows the samples' composition, measured thickness and calculated density. All samples are cast cylindrically and have same diameter of 10.1-10.2 cm and same thickness of 20.3 cm.

Table 8 Grancrete™ concrete HFR samples tested for γ -ray attenuation

Sample Number	Grancrete ID	Sample Mixture	Diameter (cm)	Length (cm)	Weight gm	Calculated* Density gm/cm ³
1	HFR	HER	10.2	20.3	3542	2.135312
4	HFR + Boron Stone	HFR and Boron Stone	10.1	20.3	3552	2.183953
5	HFR + Pb + Stone	HFR and lead shots + Stone	10.1	20.3	4532	2.786508
Control 1	Grancrete	Standard Portland	15.0	28.5	11113.013 1	2.206549
Control 2	Grancrete Trial 2	Standard Portland	15.0	28.0	10432.624 5	2.108444

*Literature indicates 2.25g/m³ for standard concrete

9.3 Experimental Results of Grancrete™ HFR Samples:

Test 1

The first test was conducted by first measuring the background and calibrating the detector and the instrumentation. The second step was to measure the source intensity in air at the distance that corresponds to the thickness of the samples. The third step is to measure the intensity with the sample in place. Each test was conducted for the same amount of time (30 minutes counting). The spectra of Test 1 is shown in Figure 23, in which it is clear that the measured photon counts after passing through the samples is close to the background. Calculations of the linear attenuation coefficient for Test 1 are shown in Table 9, where it is obvious that the sample with lead shots has the highest attenuation.

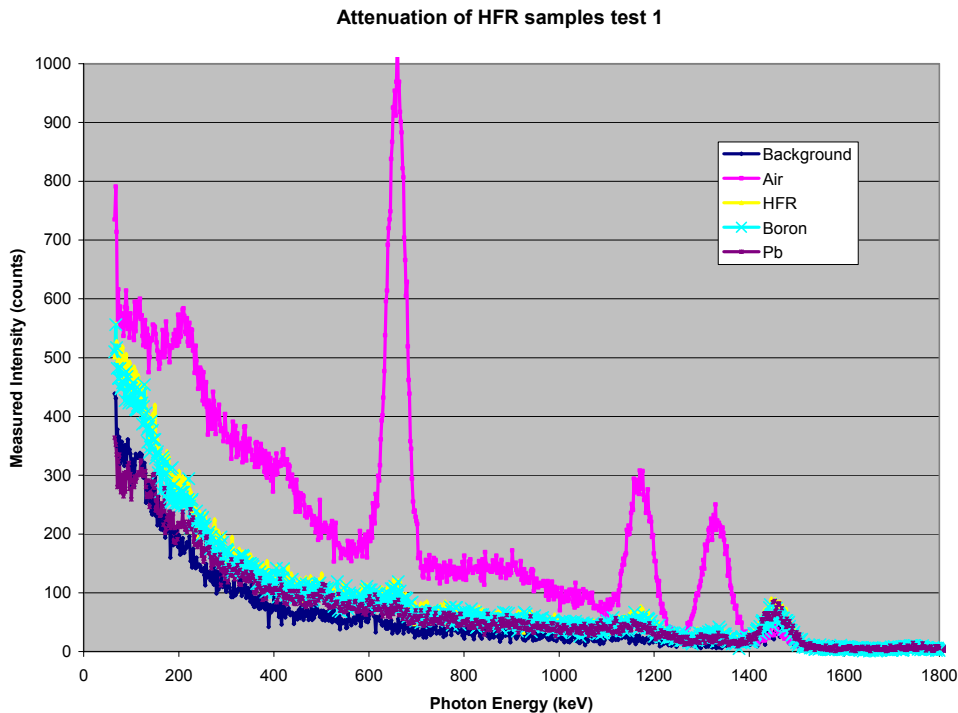


Figure 23 Measured photon spectra for Test 1 showing the background, the intensity in air and the measured intensity after γ -ray passes through the samples

Table 9 γ -ray linear attenuation coefficient of Grancrete™ concrete HFR samples Test 1

Peak Energy (MeV)	HFR μ (cm^{-1})	HFR+Boron μ (cm^{-1})	HFR+Pb μ (cm^{-1})
0.662	0.106325	0.115888	0.142428
1.173	0.078281	0.091594	0.104342
1.332	0.100030	0.112580	0.140347

Test 2

A second test was conducted with same exact procedure and the spectra of Test 2 is shown in Figure 24, in which it is also clear that the measured photon counts after passing through the samples is close to the background. Calculations of the linear attenuation coefficient for Test 2 are shown in Table 10, where it is obvious that the sample with lead shots has the highest attenuation.

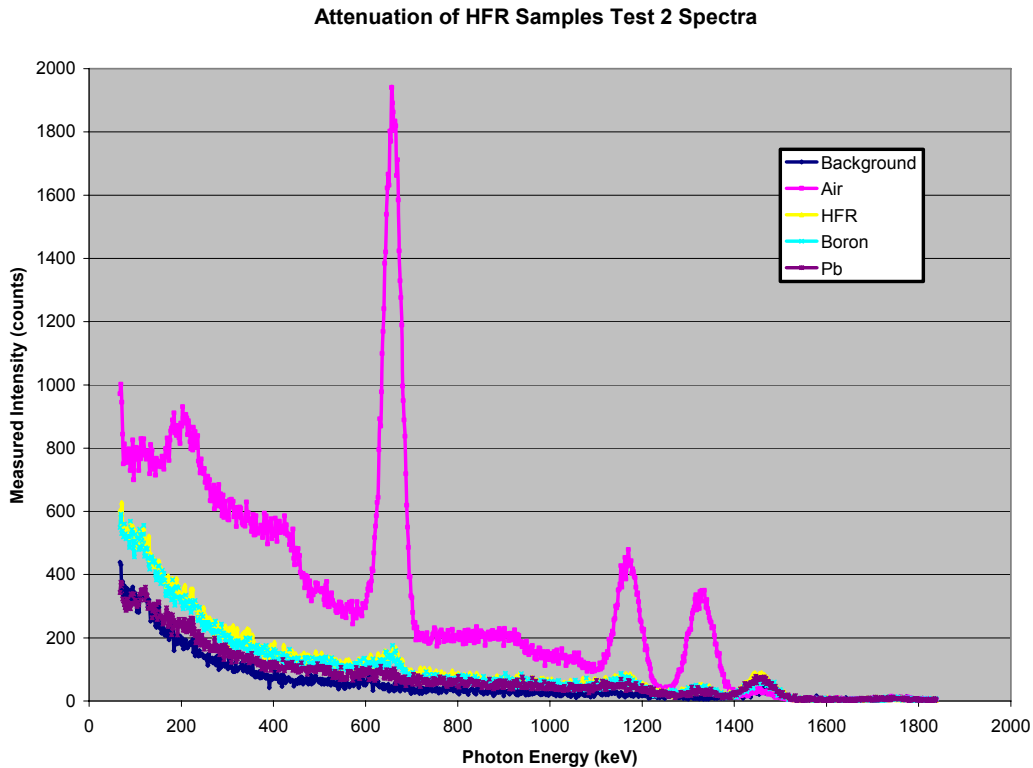


Figure 24 Measured photon spectra for Test 2 showing the background, the intensity in air and the measured intensity after γ -ray passes through the samples

Table 10 γ -ray linear attenuation coefficient of Grancrete™ concrete HFR samples Test 2

Peak Energy (MeV)	HFR μ (cm^{-1})	HFR+Boron μ (cm^{-1})	HFR+Pb μ (cm^{-1})
0.662	0.115309	0.122238	0.154135
1.173	0.087376	0.096702	0.113605
1.332	0.106713	0.111843	0.135440

Test 3

A third test was conducted on samples prepared as control, or standard, concrete samples with same exact procedure and the spectra of Test 3 is shown in Figure 25, in which it is also clear that the measured photon counts after passing through the control samples is close to the background. Calculations of the linear attenuation coefficient for Test 2 are shown in Table 11, where it is obvious that the sample with lead shots has the highest attenuation.

Attenuation Standards Samples Spectra Test 3

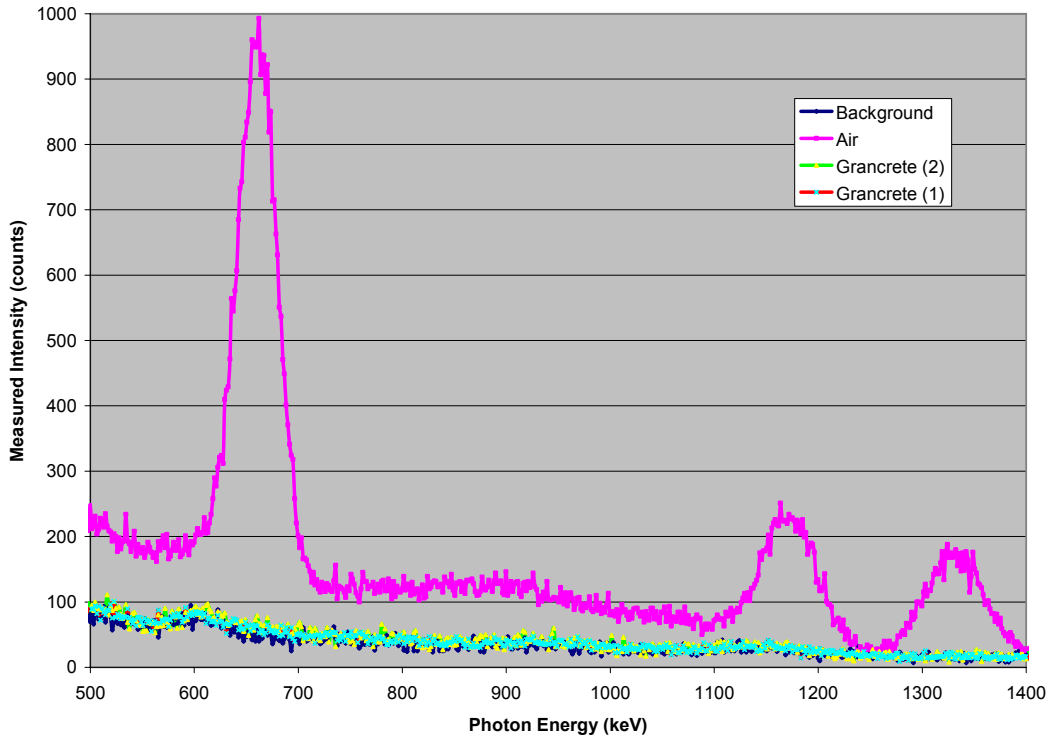


Figure 25 Measured photon spectra for Test 3 showing the background, the intensity in air and the measured intensity after γ -ray passes through the samples

Table 11 γ -ray linear attenuation coefficient of Grancrete™ control samples Test 3

Peak Energy (MeV)	Grancrete control 1 μ (cm^{-1})	Grancrete control 2 (Grancrete trial 2) μ (cm^{-1})
0.662	0.144776	0.125163
1.173	0.140047	0.136873
1.332	0.170921	0.141738

9.4 Remarks for HFR Samples:

It is reasonable to believe that the data of Test 1 and Test 2 are close to each other, however, we rely more on data of Test 2 as the counting time is extended. The data for Test 12 has consistency in sample “Grancrete control 2 (Grancrete trial 2)” while that of sample “Grancrete control 1” does not reflect expected trends. It may be that sample “Grancrete control 1” has the aggregates lined up in a different way such that the results are showing increasing attenuation coefficient with increased photon energy and it is proposed to re-test this sample. It is reasonable to believe the data of

sample “Grancrete control 2 (Grancrete trial 2)” and the discussion will be based on this sample as a control (or standard).

Table 12 shows the data for Test 1 and 2 for all samples for reason of comparison, and Table 13 shows the data for the standards, as well as the values from published literature. Ref. 1 is the Book by Lamarsh and Baratta (2001), which is the 3rd Edition published in 2001; and a recently published paper by Medhat in 2009 in which the author conducted an experiment on standard concretes (density = 2.25 g/m³) and obtained results close to calculated data. The published results in Ref. 2 are for the mass attenuation coefficient given by (μ/ρ) , where μ is the linear attenuation coefficient (cm⁻¹) and ρ is the density (g/cm³), hence one obtains the linear attenuation coefficient by multiplying the mass coefficient by the density $\mu = (\mu/\rho)\rho$, and these values are shown in Table 13.

Table 12 γ -ray linear attenuation coefficient of Grancrete™ concrete HFR samples Tests 1 and 2

Peak Energy (MeV)	HFR μ (cm ⁻¹) Test 1	HFR μ (cm ⁻¹) Test 2	HFR+ Boron μ (cm ⁻¹) Test 1	HFR+ Boron μ (cm ⁻¹) Test 2	HFR+ Pb μ (cm ⁻¹) Test 1	HFR+ Pb μ (cm ⁻¹) Test 2
0.662	0.106325	0.115309	0.115888	0.122238	0.142428	0.154135
1.173	0.078281	0.087376	0.091594	0.096702	0.104342	0.113605
1.332	0.100030	0.106713	0.112580	0.111843	0.140347	0.135440

Table 13 γ -ray linear attenuation coefficient of Grancrete™ control samples Test 3

Peak Energy (MeV)	Grancrete control 1 μ (cm ⁻¹)	Grancrete control 2 (Grancrete trial 2) μ (cm ⁻¹)	Data from Lamarsh and Baratta (2001)	Data from Medhat 2009 Measured (2009)	Data from Medhat 2009 Calculated (2009)
0.662	0.144776	0.125163	0.19	0.13725	
1.173	0.140047	0.136873	0.133	0.1305	0.13275
1.332	0.170921	0.141738	0.1215	0.11475	0.12375

-J.R. Lamarsh and A.J. Baratta, “ Introduction to Nuclear Engineering” 3rd edition, Printice-Hall, ISBN: 0-201-82498-1, (2001)

- M.E. Medhat, “Gamma-ray attenuation coefficients of some building materials available in Egypt”, Annals of Nuclear Energy, Vol. 36, pp. 849–852, (2009).

To assess the test results, the comparison will be taken for Test 2 results, Test 3 results of “Grancrete control 2 (Grancrete trial 2)”, and test results of Medhat (2009). Comparison is shown in Table 14.

Table 14 γ -ray linear attenuation coefficient of Grancrete™ concrete HFR samples Tests 1 and 2

Peak Energy (MeV)	HFR μ (cm ⁻¹) Test 2	HFR+ Boron μ (cm ⁻¹) Test 2	HFR+ Pb μ (cm ⁻¹) Test 2	Grancrete control 2 (Grancrete trial 2) μ (cm ⁻¹)	Data from Ref.2 Medhat Measured (2009)
0.662	0.115309	0.122238	0.154135	0.125163	0.13725
1.173	0.087376	0.096702	0.113605	0.136873	0.1305
1.332	0.106713	0.111843	0.135440	0.141738	0.11475

Of interest are the results of the 'HFR+Pb' sample, which shows better attenuation at photon energies of 0.662 and 1.332MeV as compared to data published by Medhat (2009), and close results to the control 2 sample, which is expected due to the inclusion of lead in the mixture. Also of interest is the sample 'HFR+Boron' at low photon energy as compared to the control 2 samples, and at the 1.332MeV photon peak as compared to data from Medhat (2009).

It may be of interest to formulate a mix that incorporates boron, which is a good neutron absorber and lead or heavy aggregates (such as granite) as a γ -ray attenuator.

9.5 Thickness Calculations and measured Densities of HFR Samples:

Table 15 shows the calculation of the HFR formulae that will attenuate the γ -ray intensity by a factor of 100 (yellow) and by a factor of 1000 (green).

The calculations were done for photon energies of 0.662, 1.173 and 1.332MeV, thus covering the entire range.

For attenuation of γ -ray intensity by a factor of 100, a 20 inch thick HFR will cover all photon energy ranges, a 18 inch thick HFR+Boron will cover the range, and a 16 inches thick HFR+Pb will cover the range.

For attenuation of γ -ray intensity by a factor of 1000, a 31 inch thick HFR will cover all photon energy ranges, a 28 inch thick HFR+Boron will cover the range, and a 24 inch thick HFR+Pb will cover the range.

Table 15 Thickness calculation of γ -ray attenuation by a factor of 100 and 1000 of HFR

μ HFR	μ Boron	μ Lead		x (cm) for HFR	x (cm) for HFR Boron	x (cm) for HFR Lead	x (inch) for HFR	x(inch) for HFR Boron	x(inch) for HFR Lead
0.115309	0.122238	0.154135	x for I/Io=0.01	39.93765868	37.67382533	29.87754417	15.72348767	14.8322147	11.76281267
0.087376	0.096702	0.113605	i.e. I/Io=100	52.70523183	47.62226906	40.53672296	20.75009127	18.74892483	15.95933975
0.106713	0.111843	0.13544	This means dropping the dropping the intensity by a factor of 100	43.15490496	41.17513138	34.00143755	16.99012006	16.21068164	13.38639274
0.115309	0.122238	0.154135	x for I/Io=0.01	59.90648802	56.51073799	44.81631625	23.5852315	22.24832204	17.644219
0.087376	0.096702	0.113605	i.e. I/Io=1000	79.05784775	71.43340359	60.80508444	31.12513691	28.12338724	23.93900962
0.106713	0.111843	0.13544	This means dropping the dropping the intensity by a factor of 1000	64.73235744	61.76269707	51.00215633	25.48518009	24.31602247	20.0795891

It has been previously shown that the attenuation coefficients of the HFR samples are compatible with recently published values, and that the HFR+ Boron and HFR+Lead are promising combination. The important fact is that the HFR samples are of less density as compared to concretes (average of 2.1g/cm³ versus 2.25g/cm³, except HFR+Pb with is close to 2.8g/m³), as shown in Table 16.

Table 16 Grancrete™ concrete HFR samples tested for γ -ray attenuation

Sample Number	Grancrete ID	Sample Mixture	Diameter (cm)	Length (cm)	Weight gm	Calculated* Density gm/cm ³
1	HFR	HER	10.2	20.3	3542	2.135312
4	HFR + Boron Stone	HFR and Boron Stone	10.1	20.3	3552	2.183953
5	HFR + Pb + Stone	HFR and lead shots + Stone	10.1	20.3	4532	2.786508
Control 1	Grancrete	Standard Portland	15.0	28.5	11113.013	2.206549
Control 2	Grancrete Trial 2	Standard Portland	15.0	28.0	10432.624	2.108444

***Literature indicates 2.25g/m³ for standard concrete**

10. Experimental Results of Grancrete™ GCI Samples:

The experimental setup is typical to the one used for the HFR samples (in section 9). Instrumentation set up is exactly the same the same radiation sources were used for the GCI samples.

Table 17 lists the Grancrete™ GCI cylindrical concrete samples tested for γ -ray attenuation. The table shows the samples' measured thickness and the calculated density. All samples are cast cylindrically and have diameter of 10.1-10.35 cm and same thickness of 20.5 except the control sample which has a thickness of 20.2 cm.

Table 17 Grancrete™ concrete HFR samples tested for γ -ray attenuation

Sample Number	Grancrete ID	Diameter (cm)	Length (cm)	Weight gm	Calculated* Density gm/cm ³
1	A	10.3	20.5	3784	2.215297
2	B	10.2	20.5	3782	2.257753
3	C	10.3	20.5	3854	2.262132
4	D	10.35	20.5	5036	2.919848
5	E (control)	10.1	20.2	3958	2.445630

*Literature indicates 2.25g/m³ for standard concrete

10.1 Experimental Results:

The test was conducted by first measuring the background, calibrating the detector and the instrumentation. The second step was to measure the source intensity in air at the distance that corresponds to the thickness of the samples. The third step is to measure the intensity with the sample in place. Each test was conducted for the same amount of time (30 minutes counting). The spectra of the test is shown in Figure 26, in which it is clear that the measured photon counts after passing through the samples is close to the background.

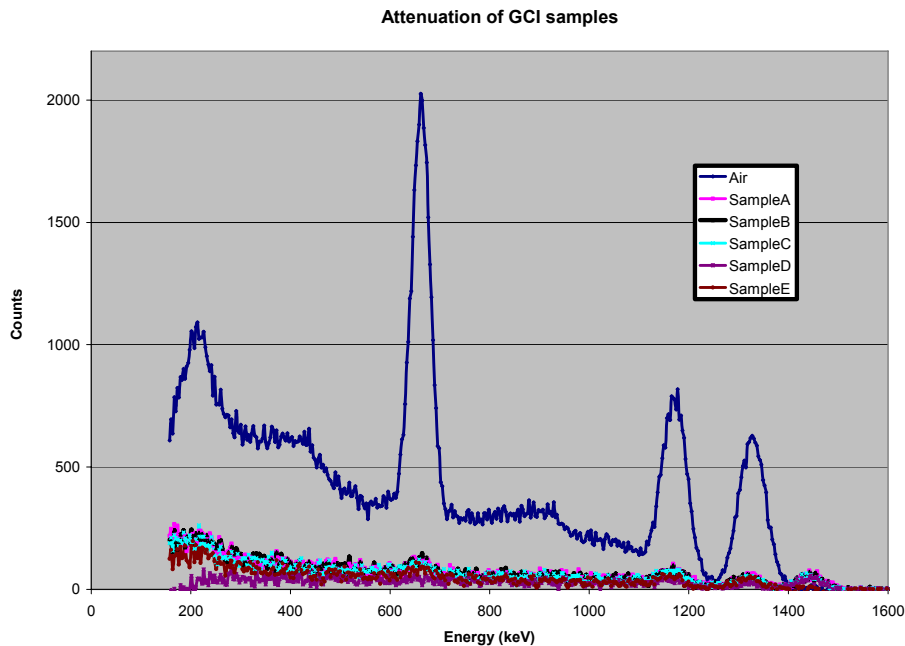


Figure 26 Measured photon spectra for GCI samples showing the background, the intensity in air and the measured intensity after γ -ray passes through the samples.

Calculations of the linear attenuation coefficients are shown in Table 18, where it is obvious that sample **D** is of better attenuation than all other samples including the control.

Table 18 γ -ray linear attenuation coefficient of Grancrete™ concrete GCI samples

Peak Energy (MeV)	Sample A μ (cm ⁻¹)	Sample B μ (cm ⁻¹)	Sample C μ (cm ⁻¹)	Sample D μ (cm ⁻¹)	Sample E μ (cm ⁻¹) Control
0.662	0.11780394	0.11807444	0.121897403	0.161134142	0.134432982
1.173	0.09764344	0.098926647	0.104402028	0.133856617	0.127765353
1.332	0.10974724	0.109781368	0.113320301	0.144873101	0.129631381

Published Attenuation coefficients of ordinary concrete are shown in Table 19 as published in 2 references, where Medhat (2009) is the most recent and has data obtained from measurements and calculations. It is clear that Sample E (control) has close values to that of Medhat (2009) “both the calculated and the measured values”, hence, one can conclude that sample **E** represents ordinary concrete to compare results to it. However, it is also worthy to compare to Medhat’s published data, and it is obvious that Sample D has higher attenuation coefficients than that of Medhat (2009).

Table 19 γ -ray linear attenuation coefficient of Grancrete™ concrete GCI samples

Energy (MeV)	Data Ref 1	Data Ref 1	Data Ref 2
	Lamarsh and Baratta	Medhat (measured)	Medhat (calculated)
0.662	0.19	0.13725	
1.173	0.133	0.13050	0.13275
1.332	0.1215	0.11475	0.12375

Of interest is to compare results for an assumed 4-inch thick concrete for all samples to evaluate the percent reduction in γ -ray intensity. Table 20 shows the percent reduction for 4-inch GCI samples, while Table 21 shows the percent reduction for data published by Lamarsh 2001 and Medhat 2009 for calculated 4-inch thickness. It is shown that sample D has the highest percent attenuation as compared to all GCI samples (including the control sample E), and better than calculated percent for same thickness of published data (Lamarsh and Medhat). Even for Lamarsh published data,

Sample D is better at the tested 2 higher energies; and better than all calculated data for Ref. 2 (for both measured and calculated data).

Table 20 Percent attenuation of GCI samples for 4-inch thickness

Energy (MeV)	A	B	C	D	Control Sample E
0.662	69.78670122	69.86962259	71.01748918	80.54610517	74.48335238
1.173	62.91869805	63.3990039	65.37951408	74.33349172	72.69488074
1.332	67.20952139	67.22088793	68.37854234	77.05134148	73.20767793

Table 21 Percent attenuation of Ref. 1 and 2 data for 4-inch thickness

Percent reduction for 4" thickness	Data Lamarsh and Baratta	Data Ref 1 Medhat (measured)	Data Ref 2 Medhat (calculated)
0.662 MeV	85.49098492	75.20330977	
1.173 MeV	74.10913546	73.44308446	74.04328908
1.332 MeV	70.90023246	68.83454761	71.55790728

For a reduction by a factor of 100, a hypothetical situation to drop by 100, i.e. high shielding, a comparison is shown in Table 22, in which an average of 12 inches of sample **D** would be sufficient.

Table 22 Percent attenuation of Ref. 1 and 2 data for 4-inch thickness

Energy (MeV)	Inch Lamarsh and Baratta 2001	Inch Medhat 2009 Measured	Inch Medhat 2009 Sample D calculated (inch)
0.662	9.542416465	13.20990257	11.25186196
1.173	13.63202352	13.8931734	13.54478527
1.332	14.92229735	15.80007955	14.65098286

10.2 Remarks for GCI Samples

Test results have shown higher attenuation for Grancrete GCI sample D over all other samples including the control sample and the recently published data by Medhat 2009.

A calculation for 4-inch thickness was completed for all samples, including the control E and the published data, which revealed a higher attenuation percentage of

Grancrete GCI sample **D** at all photon energies (except at the lower energy for Lamarsh published data)

It is of importance to determine the form(s) of the waste and its activity, also to know if the waste has resins, liquids, or mixed solids and other forms.

11. Investigation of Magnetization Effects of Molded Grancrete Composed Concretes

11.1 Introduction

Magnetization, which results from the response of a material to an external magnetic field, is the density of magnetic moments per unit volume. A material may respond to magnetic field if the material is ferromagnetic or contains components that respond to external magnetic fields. Magnetization can also result from any unbalanced magnetic dipole moments within the material.

The relation between the magnetic flux density B (also called magnetic induction) and the magnetic field intensity H (also called magnetic field strength) is determined by the permeability m of the material, such that $B = \mu H$.

The relation between the magnetic flux density B and the conduction current density J is given by Maxwell-Ampere's law $\nabla \times B = \mu J + \mu \varepsilon \frac{\partial E}{\partial t}$, where ε is the permittivity of the material and E is the electric field intensity. The values of m and e are material-dependent and are given by $\mu = \mu_o \mu_r$ and $\varepsilon = \varepsilon_o \varepsilon_r$, where the suffix o represents the values in free space and the suffix r represents the relative value of the material as related to free space. If there is no time-varying electric field then the equation reduces to the Ampere's law $\nabla \times B = \mu J$. The $\nabla \times B$ term represents the rotation of an induced magnetic field and thus the equation simply represents a right hand rule, which describes the direction of the force as perpendicular to the direction of the current and the magnetic field, where both current and magnetic field are orthogonal to each other.

For a material to exhibit magnetization it must have components with magnetic dipoles. Any material that does will produce or interact with magnetic and electric fields based on conditions. Materials with magnetic properties will generate electric currents when moved about in a magnetic field. If an object is immersed in a magnetic field, allowed to move, and does not produce a current, it has no magnetic properties. Additional to current production, magnetic materials will disrupt magnetic fields they are placed in or near. The magnetic flux density of the fields will be disturbed and can also be measured to test for magnetization.

Grancrete™ has developed various forms of concretes for special applications. In some applications, it is desired that these concrete mixes do not exhibit any

magnetization and hence a test was established to evaluate if any of these desired mixes would have any magnetization.

11.2 Samples Tested for Magnetization

Three samples of molded concretes were prepared; each sample with 2 metal rods made of copper as a non-magnetic material of high electrical conductivity. The metal leads are small rods of $\frac{1}{4}$ inch diameter copper embedded in the samples at each side, about 1-inch inside and 1-inch outside. These leads allow for electrical connections to measure any induced current when immersed in a magnetic field. Figure 27 shows a schematic of the molded samples with metal rods. These samples are:

Sample 1: PCW

Sample 2: PCW + SAND, ratio 1:1

Sample 3: PCW + SAND, ratio 2:1

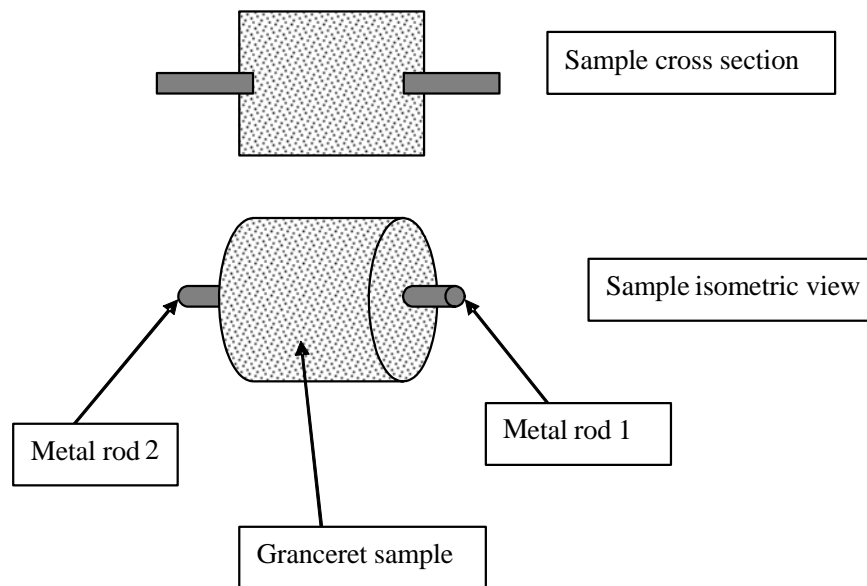


Figure 27 Schematic of the molded samples with metal rods

Four samples were also molded but without metal rods, these samples were used in a test to review if a magnetic field would be disturbed when these samples are introduced into the field. These samples are:

Sample 1A: PCW

Sample 1B: PCW + SAND, ratio 2:1

Sample 1C: PCW + SAND+PG, ratio 25:15:60

Sample 1D: PCW + SAND+GRAN, ratio 25:15:60

11.3 Magnetization Experimental Arrangement

A magnet with large bore diameter was used to generate magnetic field on axis, the magnet was powered by a LAMPDA power supply model LT-821 (0-7.5 volts, up to 300 Amps at 40°C). The axial magnetic field was monitored by a digital Gauss meter, Model GM1A Applied Magnetic Laboratory Inc., with the Hall probe of the Gauss meter installed inside the magnet bore to continuously measure the axial magnetic field. GrancreteTM samples with metal conductors were connected to an Omega Engineering digital multimeter model HHM32 to measure the electric current flowing through the samples. Figure 28 shows a schematic of the experimental arrangement

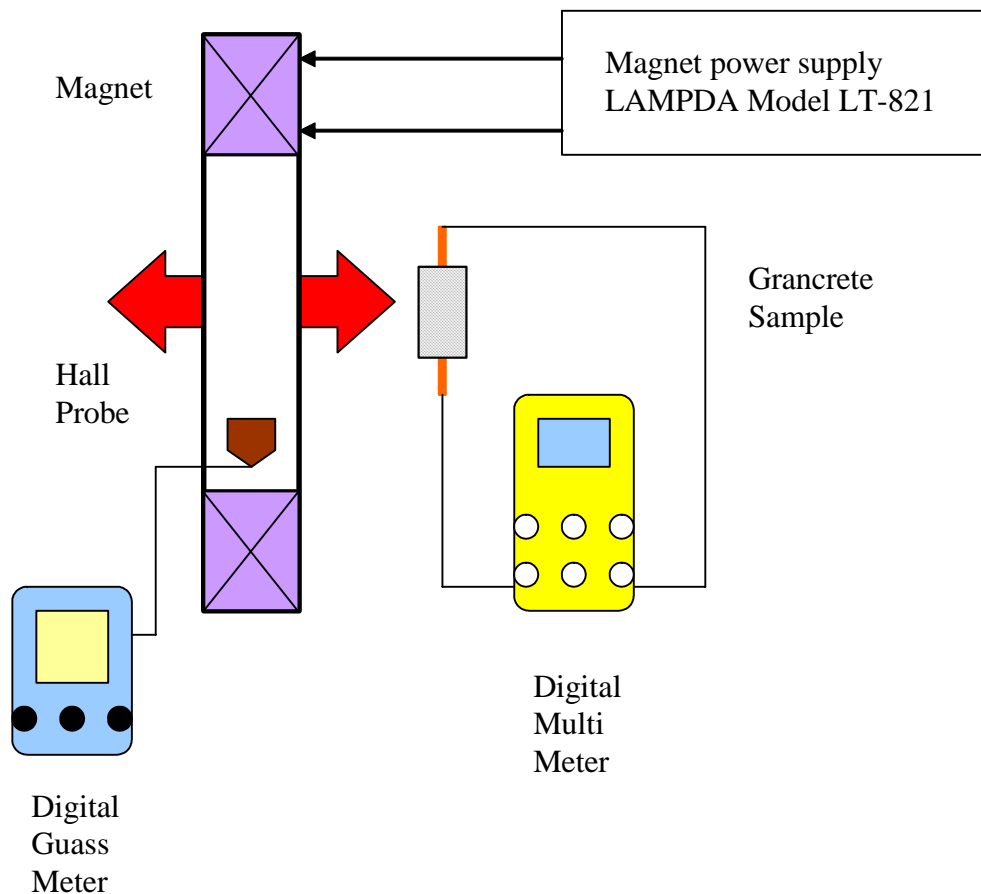


Figure 28 Schematic of the experimental arrangement to test magnetization of the samples, the red arrow shows the direction of motion of the samples in and out of the magnet bore

For each sample with metal connectors, the electrical resistance was measured prior to experimentation, and samples were tested for conductivity by connecting them to the current power supply to determine if any electric current can pass through.

The magnet was powered and adjusted for an axial magnetic field of 100 Gauss. Samples were moved inside the magnet bore and the Gauss meter reading was observed for any changes while moving the sample in and out the magnetic field. The multi meter was on continuous monitoring to observe if any electric current was generated and passed through the samples.

11.4 Magnetization Test Results

Test results are shown in Table 23 showing measured static electric resistance, static and dynamic electric current test and magnetic field intensity. The static electric resistance provides a measure of the electrical conductivity of the sample. Open circuit indicates that the sample is of high resistance such that it is not passing electric current, i.e. an insulating material. The static electric current test measures if the current flows through the sample; the test uses a steady state current source. The dynamic electric current test uses alternating current source to also measure if the current flows through the sample, it is a measure of any dynamic conductivity. The magnetic intensity test is a test in which the sample is immersed in a steady state magnetic field while the field intensity is monitored by a Gauss meter to observe any disturbance of the field due to insertion of the sample, the sample also is moved inside the field to test if any induction may take place.

Table 23 Test results are shown in Table 23 showing measured static electric resistance, static and dynamic electric current test and magnetic field intensity.

Sample	Static electric resistance	Static electric current test	Dynamic electric current test	Effect on magnetic field intensity
Samples with metal connectors				
Sample 1: PCW	Open circuit	No current flow	No current flow	No disturbance to magnetic field
Sample 2: PCW + SAND, ratio 1:1	Open circuit	No current flow	No current flow	No disturbance to magnetic field
Sample 3: PCW + SAND, ratio 2:1	Open circuit	No current flow	No current flow	No disturbance to magnetic field

Samples without metal connectors				
Sample 1A: PCW	N/A	N/A	N/A	No disturbance to magnetic field
Sample 1B: PCW + SAND ratio 2:1	N/A	N/A	N/A	No disturbance to magnetic field
Sample 1C: PCW + SAND+PG ratio 25:15:60	N/A	N/A	N/A	No disturbance to magnetic field
Sample 1D: PCW + SAND+GRAN ratio 25:15:60	N/A	N/A	N/A	No disturbance to magnetic field

11.5 Remarks on Magnetization Test Results

Results have shown that the tested samples did not alter or disturb the magnetic field. Additionally these samples do not have any dynamic current flowing through them during insertion into the magnetic field. Static tests have shown no current to flow through the samples and the electric resistance is 'open circuit' indicating the samples are nonconductive.

References:

1.	M.F.Kaplan, "Concrete Radiation Shielding", Longman Scientific and Technology, Longman Group UK Limited, Essex, England, (1989).
2.	J. R. Lamarsh and A. J. Baratta, "Introduction to Nuclear Engineering ", 3th edition , Prentice Hall, (2001).
3.	I. Akkurt, C. Basyigit, S.Kilincarslan and B. Mavi, "The Shielding of γ - Rays by Concrete Produced with Barite", Progress in Nuclear Energy, Vol. 46, No. 1, pp. 1-11, (2005).
4.	J. Wood, "Computational Methods in Reactor Shielding, Pergamon Press, Gaithersburg. MD 20899 USA (1982).
5.	N. Singh, K. J. Singh , K.Singh and H. Singh, "Gamma-Ray Attenuation Studies of PbO-BaO-B ₂ O ₃ Glass System", Radiation Measurements, Vol. 41, No. 1, pp. 84-88, Jan. , (2006).
6.	B. Goswami and N. Chaudhari, "Measurements of Gamma-Rays Attenuation Coefficients", <i>Phys. Rev.</i> 7 , pp. 1912–1916, (1973).
7.	K. Singh, R. Kaur, Vandana, V. Kumar, "Study of Effective Atomic Numbers and Mass Attenuation Coefficients in some Compounds". <i>Rad. Phys. & Chem.</i> Vol. 47, No. 4, pp. 535–541, (1996).
8.	U. Turgut, O. Simsek, E. Buyukkasap and M. Ertugrul, "X-Ray Attenuation Coefficients at Different Energies and Validity of the Mixture rule for Compounds Around the Absorption Edge", <i>Spectrochim. Acta B</i> 57 , pp. 261–266, Feb., (2002).
9.	A. H. El-Kateb, R.A.M. Rizik, A. M. Abdul-Kader, "Determination of Atomic Cross-Sections and Effective Atomic Numbers for some Alloys", <i>Ann. Nucl. Energy</i> Vol. 27, No. 14, pp. 1333–1343, Sep. (2000).
10.	J.F. Krocher, R.E. Browman, "Effects of Radiation on Materials and Compounds", Reinhold, New York, (1984).
11.	H. Singh, K. Singh, L. Gerward, K. Singh, H. S. Sahota, R. Nathuram, " <i>Beam Interactions with Materials and Atoms</i> ", <i>Nucl. Instr. and Meth. in Phy. Res. Sec. B</i> , Vol.207, No.3, pp. 257-262, Ju., (2003).
12.	S.J.M. Allen, "Mean Values of the Mass Attenuation Coefficients of the Elements", Appendix IX. In: A.H. Compton and S.K. Allison, Editors, <i>X-rays in Theory and Experiment</i> , Van Nostrand, New York , pp. 799–806, (1935).
13.	C.M. Davison and R.D. Evans, "Gamma-Ray Absorption Coefficients", <i>Rev. Mod. Phys.</i> Vol. 24, pp. 79–107, (1952).
14.	G.R. White Grodstein, " X-Ray Attenuation Coefficient from 10 KeV to 100 MeV", NBS Circular 583, (1957).
15.	J.H. Hubbell and M.J. Berger, "Attenuation Coefficients Energy Absorption Coefficients, and Photon Atomic Cross Sections", R.G.

	Joeger, <i>Engineering Compendium on Radiation Shielding</i> , Springer Editor, Berlin, Vol.1, pp. 167–202, (1968).
16.	J.H. Hubbell, "Photon Mass Attenuation Coefficients and Energy Absorption Coefficients from 1 KeV to 20 MeV", <i>The Int. J. Appl. Radiat. Isot.</i> Vol.33, No.11, pp. 1269–1290, (1982).
17.	M.J. Berger and J.H. , Hubbell, " XCOM: Photon Cross Sections on A Personal Computer", National Bureau of Standards, NBSIR 87-3597 , Gaithersburg MD 20899, July, (1987).
18.	J.H. Hubbel and S.M. Seltzer. Report NISTIR 5632, National Institute of Standards and Technology, Gaithersburg, MD 20899, (1995).
19.	I.I. Bashter, "Radiation Attenuation and Nuclear Properties of High Density Concrete made with Steel Aggregates, Radiatin Effect and Defects in Solids" , Amisterdam, The Netherlands, (1996).
20.	I.I. Bashter , A.S. Makarious, , A. El-sayed Abdo, "Investigation of Hematite-Serpentine and Ilmenite Limonite Concretes for Reactor Radiation Shielding ", <i>Ann. of Nucl. Energy</i> , Vol. 23, No. 1, pp. 65-71, (1996).
21.	A.S. Makarious, I.I. Bashter, A. El-sayed Abdo, M. samir Abdel Azim and W. A. Kansouh, " On the Utilization of Heavy Concrete for Radiation Shielding", <i>Ann. of Nucl. Energy</i> , Vol. 23, No.3, pp. 195-206, (1996).
22.	I.I. Bashter, "Calculation of Radiation Attenuation Coefficients for Shielding Concrete", <i>Ann. of Nucl. Energy</i> , Vol. 24, No.17, pp. 1389-1401, Nov., (1997).
23.	I. Akkurt, S. Kilincarslan and C. Basyigit , "The Photon Attenuation Coefficients of Barite, Marble and Limra ", <i>Ann. of Nucl. Energy</i> , Vol. 31, No.5, pp.577-582, Mar., (2004).
24.	A. S. Makarious, I. I. Bashter and A. M. I. Kany, "Radiative Capture γ -rays Arising from Iron Fiber Additions to Ilmenite Limonite Concrete Shields, <i>Ann. nucl. Energy</i> , Vol. 15, No. 10/1 I, pp. 513-521, (1988).
25.	A. El-Sayed Abdo, "Calculation of Cross-Sections for Fast Neutrons and Gamma –Rays in Concrete Shields", <i>Ann. of Nucl. Energy</i> , Vol. 29, No.16, pp. 1977-1988, Nov., (2002).
26.	A. El-Sayed Abdo , M.A.M. Ali and M.R. Ismail, "Natural Fiber High-Density Polyethylene and Lead Oxide Composites for Radiation Shielding" , <i>Rad. Phys. and chem.</i> , Vol. 66, No. 3, pp. 185-195, Mar., (2003).
27.	A. El-Sayed Abdo, M. A. M. Ali, M. R. Ismail, "Influence of Magnetite and Boron Carbide on Radiation Attenuation of Cement-Fiber/Composite", <i>Ann. of Nucl. Energy</i> , Vol. 30, No. 4, Mar. pp.391-403,Mar. (2003).
28.	M. I. Awadallah and M.A. Imran, "Experimental Investigation of γ -Ray Attenuation in Jordanian Building Materials Using HPGe-Spectrometer", <i>J. of Env. Radioactivity</i> , Vol. 94, No. 3, pp.129-136,

	May, (2007).
29.	X. F. Gao , C. M. Tam and W. Z. Gao, “Polymer Cement Plaster to Prevent Radon Gas Contamination within Concrete Building Structures “, <i>Buil. And Env.</i> , Vol. 37, No.4, pp.357-361, Apr., (2002).
30.	U. S. Camli and B. Binici, “Strength of Carbon Fiber Reinforced Polmers Bonded to Concrete and Masonry”, <i>Constructure and Building Materials</i> , Vol. 21, No. 7, pp.1431-1446, Jul., (2007).
31.	B.Benmokrane, O. Chaallal and R. Masmoudi, “Glass Fiber Reinforced Plastic (GFRP) Rebar’s for Concrete Structures”, Vol. 9, No. 6, pp. 353-364, Dec., (1995).
32.	R. Griffiths and A. Ball, “ An Assessment of the Properties and Degradation Behavior of Glass-Fiber-Reinforced Polyester Polymer Concrete”, <i>Composites Science and Technology</i> , Vol. 60, No. 14, PP. 2747-2753, Nov. (2000).
33.	J.M.L.Reis and A.J.M. Ferreira, “Fracture Behavior of Glass Fiber Reinforced Polymer Concrete”, <i>Polymer Testing</i> , Vol. 22, No.2, Apr., (2003).
34.	A. Hosny, H. Shaheen, A. Abdelrahman, T. El-Afandy, “Performance of Reinforced Concrete Beams Strengthened by Hybrid FRP laminates”, <i>Cement and Concrete Composite</i> , Vol. 28, pp. 906-913, (2006).
35.	ASTM C637
36.	ASTM C638
37.	ACI 211.1-81
38.	Radiation Measurement Laboratory, Manual written by Drs. Robert M. Mayo and Douglas E. Peplow, NCSU, Nuclear Engineering, (2000).
39.	M.E. Medhat, “Gamma-ray attenuation coefficients of some building materials available in Egypt”, <i>Annals of Nuclear Energy</i> , Vol. 36, pp. 849–852, (2009).

Appendix 1

Physical and Mechanical Properties of Test Groups (A) and (B)

Physical and Mechanical Properties of Grancrete Group “A” after 28 Days			
Testing performed by ASTM Certified Laboratory			
ASTM Test	Protocol #	GC-A	Laboratory
Thermal Conductivity (w/m.k)	ASTM C882	0.53	Argonne Labs
Freeze Thaw Resistance	ASTM C157	81%@300 Cycles	
Water Absorption	ASTM	<1%	
pH Resistance	ASTM	No Effect: 3 to 11	
Compressive Strength (psi)	ASTM C109	~7000	
Flexural Strength (psi)	ASTM C78	~1700	
Fracture Toughness (mgm)	ASTM	0.6 to 0.7	

Compressive Strength for Grancrete “A” with Different Water per cent				
ASTM Test	Protocol #	*Flowability %	Set Time (min)	Lab
Compression Strength (psi) (3 Days)	ASTM C109	ASTM C1437	Touch	PSI-FI
@ 13% Water	8100	24	7.3	
@ 14% Water	8140	68	7.8	
@ 15% Water	8380	84	8.0	
@ 16% Water	8540	108	9.0	
@ 17% Water	8690	140	9.0	
@ 18% Water	8420	>160	9.0	
@ 19% Water	8430	>160	9.0	
@ 20% Water	8420	>160	9.3	
@ 24% Water	4500	>160	9.8	
@ 28% Water	3270	>160	9.8	

* Flowability – Workable range 60% to 120%, optimal = 100%

Physical and Mechanical Properties of Grancrete Group “B” after 28 Days			
Testing performed by ASTM Certified Labs			
ASTM Test	Protocol #	GC-B	Laboratory
Length Change (%)	ASTM C157		TEC Labs
28 days (soak/dry)		0.111%	
56 days (soak/dry)		-0.024%	
Coefficient of Thermal Expansion (1/°C)	ASTM 531	8.975E-06	TEC Labs
Modulus of Elasticity (psi)	ASTM C469	1,615,000	TEC Labs
Flexural Strength (psi)	ASTM C78	455	TEC Labs
Splitting Tensile Strength (psi)	ASTM C496		TEC Labs
7 days		185	
28 days		TBD	
Slant Bond Strength (psi)	ASTM C882		TEC labs
1 day		1350	
7 days		1220	
Direct Tensile Strength (psi)	ASTM C190		TEC Labs
1 day		285	
7 days		260	
28 days		270	
ICRI Pull-off Test (psi)	ICRI 3739		TEC Labs
1 day		205	
7 days		240	
14 days		*154	
28 days		*125	
pH Resistance	ASTM D1308		TEC Labs
pH = 0.25		Significant scarring	
pH = 3.0		No effect	
pH = 5.0		No effect	
pH = 10.0		No effect	

Compressive Strength for Grancrete "B" with Different Water per cent				
ASTM Test	Protocol #	*Flowability %	Set Time (min)	Lab
Compression Strength (psi) (3 Days)	ASTM C109	ASTM C1437	Touch	PSI-FI
@ 14% Water	8370	16	9.3	
@ 15% Water	11310	72	9.3	
@ 16% Water	12590	84	9.3	
@ 17% Water	11390	102	9.3	
@ 18% Water	11230	106	9.3	
@ 19% Water	10040	111	9.5	
@ 20% Water	9600	130	10.0	
@ 21% Water	8340	148	11.3	
@ 22% Water	6410	>160	12.0	

* Flowability – Workable range 60% to 120%, optimal = 100%

ASTM Data for Grancrete B + VR (1:1) (Steel Plate)				
Testing performed by ASTM Certified Laboratory				
ASTM Test	Protocol #	GC-B + VR	Laboratory	
Modified Fire Rating (Hrs)	ASTM E 119		VTEK Labs	
1.5" Sample Fire Rating		>3 Hrs		
ASTM Data for Grancrete B + Sand (1:1)				
Testing performed by ASTM Certified Labs				
ASTM Test	Protocol #	*Flowability %	Set Time (min)	Lab
Compression Strength (psi) (3 Days)	ASTM C109	ASTM C1437	Touch	PSI-FI
@ 9% Water	9370	24	9.0	
@ 10% Water	7680	51	9.0	
@ 11% Water	5970	82	10.0	
@ 12% Water	4800	88	10.5	
@ 13% Water	3720	117	11.0	
@ 14% Water	2990	124	11.0	
@ 15% Water	2360	>160	11.5	

- Flowability – Workable range 60% to 120%, optimal = 100%

ASTM Data for Grancrete B + Sand (2:1)			
Testing performed by ASTM Certified Laboratory			
ASTM Test	Protocol #	GC-B + Sand	Laboratory
Length Change (%)	ASTM C157		TEC Labs
28 days (soak/dry)		0.024%	
56 days (soak/dry)		-0.113%	
Flexural Strength (psi)	ASTM C78		TEC Labs
7 days		395	
28 days		670	
Splitting Tensile Strength (psi)	ASTM C496		TEC Labs
7 days		365	
28 days		465	
Slant Bond Strength (psi)	ASTM C882		TEC Labs
1 day		460	
7days		650	

ASTM Data for Grancrete B + Sand (2:1)			
Testing performed by a ASTM Certified Laboratory			
ASTM Test	Protocol #	GC-B + Sand	Laboratory
Direct Tensile Strength (psi)	ASTM C190		TEC Labs
1 day		170	
7 days		160	
28 days		195	
pH Resistance (28 Days)	ASTM D1308		TEC Labs
pH = 0.25		Significant scarring	
pH = 3.0		No effect	
pH = 5.0		No effect	
		No effect	
Freeze Thaw Resistance	ASTM C666		TEC Labs
158 cycles		92%	
309 cycles		89%	
Flame Spread	ASTM 84		VTEC Labs
Fire/Smoke		0/20	
Overall Rating		Class A	

ASTM Data for Grancrete B + Sand (2:1)				
Testing performed by ASTM Certified Labs				
ASTM Test	Protocol #	*Flowability %	Set Time (min)	Lab
Compression Strength (psi) (3 Days)	ASTM C109	ASTM C1437	Touch	PSI-FI
@ 10% Water	5640	<10	8.8	
@ 11% Water	10730	42	8.8	
@ 12% Water	9360	68	9.5	
@ 13% Water	8040	88	9.5	
@ 14% Water	6920	108	9.5	
@ 15% Water	6290	128	9.3	
@ 16% Water	4970	148	10.3	
@ 17% Water	3950	>160	12.0	
@ 18% Water	3160	>160	13.3	

- Flowability – Workable range 60% to 120%, optimal = 100%

ASTM Data for Grancrete HFR			
Testing performed by ASTM Certified Labs			
ASTM Test	Protocol #	GC HFR	Laboratory
Compressive Strength (psi) @ 20% Water	ASTM C109		CFL
1 Hour		4238	
3 Hours		6361	
1 Day		6574	
3 Days		7257	
7 Days		7419	
14 Days		8197	
28 Days		8380	
90 Days		10,750	
Compressive Strength (psi) @ 25% Water	ASTM C109		CFL
1 Hour		2683	
3 Hours		3468	
1 Day		3584	
3 Days		3949	
7 Days		4546	
14 Days		5628	
28 Days		6100	
90 Days		6400	
ASTM Data for Grancrete HFR			
Testing performed by ASTM Certified Labs			
ASTM Test	Compression Strength	*Flowability	Laboratory
ASTM C109 & C1437 (3 Days)	(psi)	(%)	CFL
@ 17% Water	9868	21	
@ 18% Water	8925	88	
@ 19% Water	8852	88	
@ 20% Water	8575	101	
@ 21% Water	6328	124	
@ 22% Water	4797	119	
@25% Water	4444	150	
@28% Water	3357	>160	
@30% Water	2766	>160	
@33% Water	1381	>160	
@35% Water	1107	>160	

* Flowability – Workable range 60% to 120%, optimal = 100%

ASTM Data for Grancrete HFR				
Testing performed by ASTM Certified Labs				
ASTM Test	Protocol #	GC HFR		Laboratory
Setting Time (Min)	ASTM C403	Initial	Final	CFL
20% Water		8.5	9.1	
25% Water		9.7	10.7	

ASTM Data for Grancrete HFR				
Testing performed by ASTM Certified Labs				
ASTM Test	Protocol #	GC HFR		Laboratory
Flexural Strength (psi)	ASTM C403	20% W	25% W	CFL
1 Hour		320	---	
3 Hours		788	501	
1 Day		1109	776	
3 Days		1195	994	
7 Days		1312	1275	
14 Days		1077	977	
28 Days		1053	1144	

ASTM Data for Grancrete HFR				
Testing performed by ASTM Certified Labs				
ASTM Test	Protocol #	GC HFR		Laboratory
Modulus of Elasticity (psi)	ASTM C496	20% W	25% W	CFL
3 Hours		400,000	200,000	
1 Day		1,400,000	1,100,000	
3 Days		1,800,000	1,200,000	
7 Days		1,800,000	1,400,000	
14 Days		1,900,000	1,500,000	
28 Days		TBD	TBD	

ASTM Data for Grancrete HFR + VR (1:1) (Steel Plate) Testing performed by ASTM Certified Laboratory			
ASTM Test	Protocol #	HFR-VR	Laboratory
Modified Fire Rating (Hrs)	ASTM E 119		VTEK Labs
1" Sample Fire Rating		2.7 Hrs	

ASTM Data for Grancrete PCW			
Testing performed by ASTM Certified Laboratory			
ASTM Test	Protocol #	GC-PCW	Laboratory
Compressive Strength (psi)	ASTM C109		CFL
1 Day		4855	
17 Days		8247	
Flexural Strength (psi)	ASTM C78		PSI-Pitt
3 Days		940	
7 Days		995	

ASTM Data for Grancrete PCW				
Testing performed by ASTM Certified Labs				
ASTM Test	Compression Strength	*Flowability Set Time	(min)	Lab
ASTM C109 & C1437 (3 Days)	(psi)	(%)	Touch	PSI-FI
@ 17% Water	10,270	<10	7.5	
@ 18% Water	10,670	<10	7.8	
@ 19% Water	11,550	76	7.8	
@ 20% Water	10,580	80	8.0	
@ 21% Water	9890	91	7.0	
@ 22% Water	9310	99	7.5	
@ 24% Water	8410	128	8.3	
@26% Water	7730	152	8.5	
@28% Water	6190	>160	9.3	
@30% Water	5210	>160	10.3	

* Flowability – Workable range 60% to 120%, optimal = 100%

ASTM Data for Grancrete PCW			
Testing performed by ASTM Certified Laboratory			
ASTM Test	Protocol #	GC-PCW	Laboratory
Hydraulic Conductivity (Perms)	ASTM D5084	1.5 X10 ⁻⁹	PSI-FI
Water			
Oil	ASTM D5084	5 X 10 ⁻⁸	PSI-FI

ASTM Data for Grancrete PCW + Sand*			
Testing performed by ASTM Certified Laboratory			
ASTM Test	Protocol #	GC-PCW + Sand	Laboratory
Shear Strength (psf) on ICF Block	ASTM		PSI-FI
3 Days @ 1:1		2606	
3 Days @ 1:2		2268	
Pull Off Bond Strength (psf) on ICF Block	ASTM		PSI-FI
3 Days @ 1:1		1909	
3 Days @ 1:2		1919	

*Sand =30/50

ASTM Data for Grancrete PCW + Sand (1:1)			
Testing performed by ASTM Certified Laboratory			
ASTM Test	Protocol #	GC-PCW	Laboratory
Hydraulic Conductivity-Water (Perms)	ASTM D5084	1.2 X10 ⁻⁸	PSI-FI
Water			
Oil	ASTM D5084	2.1 X10 ⁻⁷	PSI-FI

ASTM Data for Grancrete PCW + Slate*			
Testing performed by ASTM Certified Laboratory			
ASTM Test	Protocol #	GC-PCW + Slate (1:1)	Laboratory
Compressive Strength (psi)	ASTM C109		PSI-FI
1 Day		3367	
3 Days		3466	

*
Slate
Powder

ASTM Data for Grancrete PCW + Sand (2:1)				
Testing performed by ASTM Certified Labs				
ASTM Test	Compression Strength	*Flowability	Set Time (min)	Lab
ASTM C109 & C1437 (3 Days)	(psi)	(%)	Touch	PSI-FI
@ 10% Water	2570	<10	10.0	
@ 11% Water	6470	<10	9.8	
@ 12% Water	11960	44	9.5	
@ 13% Water	11230	82	9.0	
@ 14% Water	9180	88	9.0	
@ 15% Water	8770	100	9.5	
@ 16% Water	8720	116	9.8	
@17% Water	8000	120	10.0	
@18% Water	7508	148	10.3	
@19% Water	7230	>160	9.8	
@20% Water	6650	>160	9.8	

* Flowability – Workable range 60% to 120%, optimal = 100%

Compression Strength (ASTM C109) Grancrete PCW + Sand + Course Aggregate* Testing performed under ASTM Protocols									
				Data Source: Black = GCI Red = CFL					
Mix Design (% of each)				Compression Strength (psi)					
				1 Hr	2H	3H	1 Day	3 Days	7 Days
PCW	Sand	CA	H ₂ O [#]						
100	0	0	19					11550	
67	33	0	19					11230	
50	50	0	26					6550	
30	10	60*	24	4826	5588	5630	5631		
25	15	60*	26	3876	4387	5090	4564		
25	20	55*	26	3241	3910		3999		
25	25	50*	26	3535	3328		3475		
20	20	60*	26	2949	3303		4906		
20	20	60**	26		4359				
17	23	60*	26			3431			
30	20	50***	25				2269	2154	
# Water ratio to PCW				*Pea Gravel		**Granite Stone: ½(-)		*** Shale: 3/8 (-)	

ASTM Data for Grancrete PCW + Large/Fine Aggregate*			
Testing performed by ASTM Certified Laboratory			
ASTM Test	Protocol #	7 Day compression Strength (psi)	Laboratory
Compressive Strength (psi)	ASTM C109		U. Maine
PCW Only		4270	
PCW + Large Agg (1:2)		5130	
PCW + Fine Agg (1:2)		5040	
PCW + Large Agg + Fine Agg (1:2:1)		5705	

*Large Aggregate = 3/4"; Fine Aggregate = 1/4- (gravel)

Compression Strength (ASTM C109) Grancrete PCW + Sand + Course Aggregate* Testing performed under ASTM Protocols													
				Data Source: Black = GCI Red = CFL									
Mix Design (% of Each)				Compression Strength (psi)									
PCW	Sand	Agg	H ₂ O	1Hr	2H	3H	1 Day	3 Days	7 Days	14 Days	21 Days	28 Days	+90 Days
100	0	0	19					11550					
67	33	0	19					11230					
50	50	0	26					6550					
30	10	60*	24	4826	5588	5630	4630	5210	6020	8652		10137	
25	15	60*	26	3876	4387	5090	5140	5810	6680	9884			
25	20	55*	26	3241	3910		3999			8571			
25	25	50*	26	3535	3328		3475	5410	7219				
20	20	60*	26	2949	3303		3300	4310	4750	7649	8721		7681
20	20	60**	26		4359								
18	17	65*	26				3380	4710	4610				
17	23	60*	26			3431	3658						7235
				# Water ratio to PCW				*Pea Gravel: 3/8"			**Granite Stone: 1/2"		

Comparison of Lab Mixing and Volumetric Truck Mixing for Grancrete PCW + Sand + Granite Stone (25:15:60) CFL, NCSU				
	Compressive Strength (psi)		Modulus of Elasticity (ksi)	
	6 hours	7 days	1day	7 days
Lab mixing	6260	7180	2400	2830
Truck mixer	6250	6910	3220	4110

Basic Strength Study of Grancrete PCW in Different Mix Designs Constructed Facilities Laboratory, NCSU												
Mix Design (%)		Compression Strength (psi) ASTM C39				Modulus of Elasticity (ksi)				Tensile Strength (psi)		Slump (in)
PCW- Sand- Agg	Agg size	6 Hrs	1 Day	3 Days	7 Days	6 Hrs	1 Day	3 Day	7 Days	6 Hrs	7 Days	
30-10-60	½"	2960	2630	6100	7620	2440	2090	2190	2500	401	423	9.25
25-15-60	½"	3310	2680	6830	6850	3500	2590	2710	2380	347	347	8.0
20-20-60	½"	1720	2850	3920	4750	1760	1880	2120	2650	192	192	7.5
18-17-65	½"	1880	2560	5180	6540	2660	2130	2730	2960	322	322	0
30-10-60	3/8"	1550	4630	5210	6020	2030	2220	2280	2510	318	335	9.5
25-15-60	3/8"	2290	5140	5810	6680	2380	2190	2340	2530	341	398	9.0
20-20-60	3/8"	1610	3300	4310	4750	2040	1810	2000	2320	227	290	8
18-17-65	3/8"	2070	3380	4710	4610	1710	1830	1870	2400	222	284	0.5
Water/Grancrete Ratio was constant at 25%						Aggregates = Granite stone						

Appendix 2

Photograph of sample 7B with observed cracking



Appendix 3

Photographs of different samples after compressive stress test

Photo for Sample No. 2AA after Compressive Strength Test, Civil Eng. Lab, NCSU



Photo for Sample No. 8AA after Compressive Strength Test, Civil Eng. Lab, NCSU.



Photo for Sample No. 10A after Compressive Stress Test, Civil Eng. Lab, NCSU.



Photo for Sample No. 15A after Compressive Stress Test, Civil Eng. Lab, NCSU



Photo for Sample No. 5B after Compressive Strength Test, Civil Eng. Lab, NCSU.



Photo for Sample No. 17B after Compressive Strength Test, Civil Eng. Lab, NCSU.

